

Determination of optimum specific thrust for civil aero gas turbine engines: a multidisciplinary design synthesis and optimisation

Proc IMechE Part G:

J Aerospace Engineering
227(3) 502–527

© IMechE 2012
Reprints and permissions:
sagepub.co.uk/journalsPermissions.nav
DOI: 10.1177/0954410011435623
uk.sagepub.com/jaero



Abhijit Guha¹, D Boylan² and P Gallagher²

Abstract

A systematic methodology for the determination of optimum specific thrust of civil turbofan engines is presented. The optimum is defined as the specific thrust at which the engine direct operating cost is minimised. Based on publicly available data and clean-sheet analysis, the developed method provides a rationale for the values of specific thrust found in existing engines and the basis for future designs. The optimum specific thrust determined here complements the thermodynamic optimisation strategy for engine parameters developed in a previous publication by Guha. The process of optimisation thus involves a complex multidisciplinary methodology involving aerodynamics, thermodynamics, structures, system integration, economics, legislations, and other design and operational issues. This study utilises two models: the fixed aircraft rubber engine model which simulates the retrofitting of new engines to a current airframe, and the rubber aircraft rubber engine model which simulates the thermodynamic optimisation of the engines alongside the optimisation of the airframe dimensions. Both models demonstrate that as the design range of the aircraft increases, the optimum value of specific thrust decreases. As fuel prices rise, the optimum value of specific thrust reduces further, taking it to levels where radical changes in engine design and integration would be necessary.

Keywords

Thermodynamic optimisation, aerodynamic optimisation, turbofan, direct operating cost, typical mission, specific fuel consumption, cruise specific thrust

Date received: 15 March 2011; accepted: 15 December 2011

Introduction

The aim of any engine manufacturer who wants to be competitive is to provide the lowest propulsion system cost to the airline. The engine performance is an important issue, but also important are the acquisition cost, reliability and maintainability (and satisfying legislation). The industry has therefore paid attention to cost studies. ^{1–4} Overall, in civil engines, direct operating cost (DOC) is optimised and in military engines, life cycle cost is optimised.

The calculation methods that the engine manufacturers use are proprietary information. In this article, we have developed a method of determining the optimum value of the specific thrust of a civil aircraft engine that would minimise the engine direct operating cost (EDOC). With this aim, a user-friendly general-purpose computational tool has been developed with

the acronym COST (computation of optimum specific thrust). Comprehensive data regarding existing aircraft and engines^{5–7} of all major manufacturers have been used in the database of COST which offers a flexible choice to the user about mission and configuration of the aircraft and engine. Along with comprehensive aerodynamic and aircraft design formulae available in the literature, the method encapsulates many practical insights accrued from having a major aircraft design

Corresponding author:

Abhijit Guha, Mechanical Engineering Department, Indian Institute of Technology, Kharagpur 721302, India. Email: a.guha@mech.iitkgp.ernet.in

¹Mechanical Engineering Department, Indian Institute of Technology, India ²Aerospace Engineering Department, University of Bristol, UK

[,]

project at the University of Bristol that strongly and directly involves Airbus.

Guha⁸⁻¹² formulated a new methodology for the thermodynamic optimisation of jet engines in which the optimum combination of all variables (overall pressure ratio (OPR), fan pressure ratio (FPR), bypass ratio, and burner exit temperature) is concurrently determined, which maximises the overall efficiency while maintaining the specific thrust at a predetermined value established from a DOC analysis. This is very different from the usual parametric studies available in the literature where the effects of the variation of a single variable on engine performance are calculated numerically while all other variables are kept fixed—therefore at their non-optimum levels. The economic and aerodynamic performance analysis developed in this article integrates with the thermodynamic optimisation method of Guha^{8–12} in that the output of COST would be the specific thrust at which the thermodynamic optimisation of the engine would take place.

Calculations performed by COST provide an engineering and economic rationale for the observed values of the specific thrust of current aero-engines. COST can also be employed to study the effect of variation in any particular parameter on the EDOC and for sensitivity analysis. Studies presented in this article cover a number of engine thrust requirements and mission profiles to ascertain the trends and variation in the optimum value of specific thrust. Analysis is also conducted into the variation of optimum specific thrust with fuel price to determine the effects of future oil price rises on EDOC and the possible step changes required in aero-engine design to respond to this.

Soaring prices in aviation fuel in recent years, reaching a high of \$4.30 per US gallon¹³ in July 2008, have caused fuel costs to represent an increasingly significant proportion of airline DOCs, typically in excess of 30%. This coupled with economic recession globally seen in the later quarters of 2008, has put considerable strain on airlines worldwide, ultimately forcing over 30 airlines into insolvency at the close of the year. ¹⁴ Airlines have in turn utilised numerous strategies in their attempts to alleviate the pressure of rising fuel prices. As well as fuel hedging strategies and flight plan optimisation, many airlines have turned their attention to their aircraft fleet, with the focus of their future aircraft and engine acquisitions lying very much with fuel-associated operating costs.

With the colossal costs associated with bringing an engine to market, typically estimated at over \$1 billion, 15 many large engine manufacturers have opted for the development of engine 'families'. Through scaling of the modularised components of engines, development costs can be significantly reduced, with future

family additions also benefiting from the in-service feedback of its predecessors. This methodology, though beneficial to development costs, may however, not be conducive to the optimisation of an engine for its intended in-service use.

Economic adversity, along with ever-growing environmental pressure being placed on the aerospace sector worldwide, has highlighted that incremental changes to engine design may not be sufficient in meeting the future needs of the civil aerospace market. Aero-engine manufacturers have in turn responded with extensive research into and development of a new '3rd generation' of aero-engine designs. 16 In many cases, this has been centred on 'clean-sheet' design and analysis. The application of these future engines broadly lies in two scenarios. The first is in the retrofitting of new engine designs onto existing airframes. This business model has been previously used and looks set to continue with Airbus currently conducting flight tests with Pratt & Whitney's novel geared turbofan (GTF) engine, for potential application on their existing A320 narrow body aircraft.¹⁵ The second scenario involves engine design and integration conducted in parallel with airframe design in order to achieve a more optimised system. This scenario also holds potential for the future, with research involving engine-airframe design and integration for the anticipated replacements of Boeing's 737 and Airbus's A320 families taking place.¹⁶

This article outlines the development of two robust computational models capable of calculating the optimum value of engine specific thrust for both of the aforementioned engine design scenarios. The first model, fixed aircraft rubber engine (FARE), determines optimum specific thrust for an engine to be installed on an aircraft of fixed airframe mass and geometry, simulating the engine retrofitting scenario. The second model, rubber aircraft rubber engine (RARE), performs an engine design and integration in parallel with airframe sizing for an aircraft of predetermined mission range and payload. A commercially available software for the calculation of gas turbine performance, GasTurb 10,¹⁷ is utilised in conjunction with COST in the optimisation process of each model.

Here, specific thrust has been treated as the basic design parameter. The specific thrust is a good overall indicator of the engine for the following reasons.

 It fixes the mean jet speed. Thus, it determines the propulsive efficiency, and, governs the jet noise, as the jet noise is approximately proportional to the eighth power of jet speed. Environmental considerations such as the noise level would increasingly determine the design parameters of a future jet engine.

- For a given thrust required, the specific thrust almost fixes the fan diameter and hence the size of the engine.
- 3. Thus, a given value of specific thrust largely determines the nacelle weight, price and drag.
- 4. The specific thrust determines whether the engine would satisfy any geometric constraint (for example, whether the engine could be fitted under the wing).

In order to establish the relevant range of specific thrust characteristic of the current design trend, the values of the specific thrust⁵ of several current civil turbofan engines of various manufacturers have been plotted in Figure 1. Specific thrust data in Figure 1 are slightly approximate because although net thrust is known at cruise, the mass flow rate is estimated from given values at sea level static conditions by dynamic scaling, i.e. assuming the same non-dimensional operating point.

In Figure 1 and the rest of this article, values of the cruise specific thrust have been shown. Certain parameters such as the take-off noise are related to the take-off specific thrust. For a given engine, the take-off thrust and cruise thrust are related; a numerical gas turbine performance package such as GasTurb can compute this relation. The relation between take-off and cruise thrust can also be manually determined by dynamic scaling, by assuming that the non-dimensional operating point essentially remains the same under take-off and cruise conditions. ¹⁸

Figure 1 shows that for most existing engines, the cruise specific thrust lies in the band 15–20 lbf/lbm/s. Over the past 40 years of civil engine design, the specific thrust has slowly reduced, while the bypass ratio has significantly increased from 1–2 in the 1960 s to 7–9 in the 1990 s. The trend of reducing specific thrust with time has been accompanied by technology improvements bringing reductions of installation drag and specific weight of engines. The forecast 19–22 is that the design driver for future engines might be towards even lower specific thrust. A surge in fuel price and/or the introduction of more stringent noise regulation may necessitate such designs. Future geared turbofan or

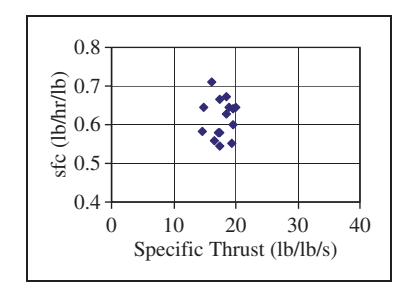


Figure 1. Data for various current civil turbofan engines under cruise conditions (typically 35,000 ft, M = 0.8-0.85).

open rotor engine would significantly reduce the specific thrust.

Figure 1 also shows sfc of various engines. Detailed data regarding OPR, B, thrust, configuration, number of stages, date of entry into service, etc. are given in Rolls-Royce Aero Data. The variation in sfc reflects the effects of these factors and evolving technology standard. Considerations of engine weight and initial price, stage length of the aircraft, fuel price, etc. influence design decisions. Following industrial practice, sfc and the specific thrust have been expressed here, respectively, in lbm/h/lbf and lbf/lbm/s, where 1 lbf/lbm/s and 1 lbm/h/lbf are equal to 9.81 m/s and 28.316×10^{-6} kg/s/N, respectively.

The design and optimisation of the aero-engine and the civil transport aircraft are complex and multidisciplinary. In the industry, typically a large team of people, a cumulative experience of many years and a body of proprietary information (not available to the public) are involved. The aim of this study is to formulate a systematic methodology to determine the optimum specific thrust of a civil aero-engine based on information available in the public domain and 'clean-sheet analysis' (the engine manufacturers, on the other hand, may have practical constraints arising from previous program investment, current product range and available in-house technologies⁸). Once the optimum specific thrust is determined, optimum values of other overall parameters such as OPR, turbine entry temperature (TET), bypass ratio (B) and FPR can be determined by the optimisation procedure developed by Guha.⁸ In order to implement the generic principle developed in this article, many specific equations, data and approaches have been adopted and sometimes simplifying assumptions have been made—these details can be found in the following descriptions and cited references. The essence of the generic principle is, however, not limited by these details and specificities. It is expected that the reader and user of this article may like to adapt or modify the details as they think fit. Nevertheless, the computations of this article demonstrate the validity of the concept of optimum specific thrust and the values of the optimum specific thrust computed here nicely tie up with actual values of existing engines (shown in Figure 1). Within the knowledge of the present authors, this is the only paper of its kind available in the public domain.

Determination of engine direct operating cost

Bennett, ¹ Jackson² and Wilde³ have shown that when the DOC is calculated at various specific thrusts, the resulting curves show a characteristic bucket shape, giving a particular value of specific thrust that

minimises the DOC. The engine design, therefore, needs to be carried out at this optimum value of specific thrust. Jackson² has presented detailed considerations on the choice of specific thrust, and Wilde³ has described very detailed design issues.

There is an optimum specific thrust for any aircraft mission and technology standard. The optimum is a function not only of the gas path performance (e.g. the thermal efficiency of the core engine) but also depends on, among other things, installation losses, weight, engine price, fuel price and effects on noise and mechanical considerations. Since some or all of these may vary with time, the determination of optimum specific thrust should be re-examined from time to time.

Full costing would require detailed knowledge about the engine and the required data might be proprietary information of engine manufacturers. However, information available in the public domain, e.g. the Association of European Airlines (AEA) parametrics, ²³ provides useful results. With this in view, we have developed a model for calculating EDOC of various aircraft engines. This comprises:

- engine price;
- nacelle price;
- fuel cost over 14 years;
- maintenance cost over 14 years;
- cost associated with any change in aircraft weight directly attributable to alteration of the engines from a datum.

The optimum specific thrust would change with various requirements of overall thrust and aircraft range. This is because the proportion of various elements to the overall cost changes depending on the overall thrust level, stage length, etc. As the range decreases and engine size reduces, the relative proportion of maintenance costs increases, due to the dependence on number of flight cycles rather than flying time. For larger, longrange engines, fuel price assumes dominance. Legislation, such as stringent noise requirements, may also dictate the choice of specific thrust.

The full details of the equations and procedures used to determine EDOC are given in the study of Boylan and Gallagher, with an earlier version given in the study of Abdul Rahman and Hassan. These are too extensive to reproduce here in full; so, we mention the salient points. Estimating the price of an engine is difficult because many factors are involved. The engine price is estimated in this study on the basis of a study performed by Jenkinson et al. In 1995, with the engine prices updated to current values through the use of a suitable gross domestic product deflator. Jenkinson et al. recommended a value factor (VF) with which the engine price in units of million dollar (\$M) can be

correlated by a straight line fit. The value factor is related to the cruise thrust (F_{cr}) expressed in lbf unit and the cruise thrust specific fuel consumption (sfc) expressed in the unit lb/(h.lbf), through the relation $VF = (F_{cr}^{0.88}/\text{sfc}^{2.58})/1000$. The actual relation used for the numerical illustrations in this article is engine price (\$M) = 0.7935VF + 1.3822. The present approach of calculating the engine price reasonably compares to an industry estimate of the engine price as a factor of airframe price.²⁷ The nacelle price is estimated by scaling the engine price with the nacelle-to-engine mass ratio.

Typical times for each segment of mission (e.g. taxi, take-off, climb, cruise and descent) are estimated for the three representative mission profiles (short, medium, and long ranges), and this allows the calculation of the utilisation of the aircraft. The AEA method²³ is followed for the determination of maintenance costs which depend on, among other variables, the number of compressor stages, sea level static thrust, labour rate and flight time. The maintenance cost has two components—material and labour costs. For a given labour rate (\$/h), the total labour cost decreases with an increase in bypass ratio (because the access to the engine becomes easier) and increases with an increase in the number of compressor stages (because the complexity increases). The material cost depends on the bypass ratio, number of compressor stages and OPR (an increase in OPR increases the stresses in the core engine, thus increasing the materials part of the maintenance cost). Both the labour and material parts of the maintenance cost increase with an increase in the sea level static thrust of the engine. The relevant formulae for calculating the maintenance costs are given in Appendix 2.

The amount of fuel required to fly the typical and maximum missions for each aircraft is calculated using a method given by Torenbeek.²⁸ The method uses a set of equations which are not reproduced in this article (since the study of Torenbeek²⁸ is easily available). The component of EDOC due to the fuel can be calculated by multiplying the price of fuel by the amount of fuel consumed over 14 years. The weight penalty due to alterations in engine design from the datum is differently applied in the FARE and RARE models, and the respective procedures are described in the appropriate places of section 'FARE and RARE computational models'.

Determination of aircraft aerodynamic characteristics, dimensions and weight, and other design issues

Profile drag coefficient of the airframe ($C_{D0,a}$)

The profile drag (i.e. the zero-lift drag) of the airframe is calculated in great detail. The total profile drag

coefficient is determined by summing the profile drag coefficients of the four main components (viz. the wings, fuselage, horizontal tail plane, vertical tail plane) and those of miscellaneous parts (e.g. belly fairing, flap track fairings, etc.) taking interference into account

$$C_{D0,a} = \sum_{i=1}^{4} C_{D0,i} + C_{D0,misc}$$
 (1)

The detailed geometrical data of the entire airframe for three representative aircraft [Boeing 737-600 (short range), 757-300 (medium range) and 777-300ER (long range)] are taken from the studies of Jackson⁶ and Jenkinson,⁷ and used for the calculation of the profile drag. The methods and equations given in the studies of Raymer,²⁹ Kroo,³⁰ Sommer and Short³¹ and Avallone et al.³² for the calculation of the drag coefficients of the various components are used. The formulae also account for compressibility and Reynolds number effects. All formulae and calculation procedure are summarised in the study of Boylan and Gallagher;²⁴ a shorter version is given in Appendix 3. For the *i*th component of the airframe, such as the wing, the profile drag coefficient $C_{D0,i}$ is calculated from

$$C_{D0,i} = kC_{f,i}S_{wet}/S_{wing} \tag{2}$$

where $C_{f,i}$ is the friction coefficient (after corrections due to Reynolds number and compressibility are applied to the incompressible result), S_{wet} the wetted surface area of the component and k the form factor which is usually calculated from complex relations. For lifting surfaces, k is often given as function of sweep angle, aircraft Mach number and thickness/chord ratio at 70% chord location.

Profile drag coefficient of the engine nacelle and pylon including interference (C_{D0e})

A method outlined in Jenkinson²⁶ for the calculation of nacelle dimensions for mixed/separate stream engines is used. These calculations provide the values for maximum nacelle diameter, nozzle diameter and total nacelle length for mixed stream engines. Bypass cowl length, core cowl length and core cowl diameter are also calculated for separate stream engines. These dimensions are dependent on engine fan diameter, the maximum operating Mach number of each aircraft, air mass flow rate at sea level static conditions, bypass ratio and OPR of each engine. This allows for the estimation of nacelle wetted area. The required height of the pylon is determined along with the length of the wing chord at the engine attachment location, allowing

for an estimation of the wetted area of the pylon. A method outlined in Airbus UK³³ allows for the calculation of the effect that the relative vertical and horizontal distances between specified points of the engine and the wing has on interference drag. Further details are given in Appendix 4. Thus, the profile drag coefficient $C_{D0,e}$ of the nacelle plus pylon can be calculated, which encompasses compressibility effects, Reynolds number effects and interference between the wing and nacelle. Summation of the profile drag for the airframe and that for the nacelle and pylon provides the profile drag for the whole aircraft (C_{D0})

$$C_{D0} = C_{D0,a} + C_{D0,e} (3)$$

Induced drag coefficient of the aircraft (C_{Di})

The lift coefficient at the start of cruise is estimated for each aircraft by considering the mission cruise speed, wing area and cruise level international standard atmospheric (ISA) conditions

$$C_L = \frac{0.97\text{MTOW.}g}{\frac{1}{2}\rho_a V_{TAS}^2 S_{wing}} \tag{4}$$

The induced drag coefficient is then calculated following Kroo,³⁰ which relates the induced drag coefficient to the wing aspect ratio, sweep and lift coefficient of each aircraft studied, including the further increase in lift-induced drag due to the effect of the fuselage on wing span loading

$$C_{Di} = [k + (0.965\pi AR)^{-1}]C_I^2$$
(5)

where $AR = b^2/S_{wing}$ and $k = ((7 \times 10^{-5})\Lambda^2 - (3 \times 10^{-4})\Lambda + 0.38)C_{D0}$. The factor 0.965 represents the fuselage interference. The induced drag constitutes a significant portion of the overall drag of an aircraft.

Total drag, thrust and air mass flow rate at cruise

The total drag coefficient of each aircraft is calculated by combining the profile, induced and wave drag coefficients

$$C_D = C_{D0} + C_{Di} + C_{DW} (6)$$

where C_{DW} is the wave drag coefficient. The wave drag results from shock waves as parts of the accelerated flow over the surfaces become supersonic. The civil aircrafts are not intended to be flown past the drag divergence Mach number, the cruise Mach number usually lies between 0.8 and 0.85. Therefore, the magnitude of

 C_{DW} is typically 5 to 10 counts (1 count = 10^{-4}) for civil aircrafts. C_{DW} may be assumed to be 0.0005 if no other details are available.²⁶

Thus, the total drag can be calculated

$$D = \frac{1}{2}\rho_a V_{\text{TAS}}^2 S_{wing} C_D \tag{7}$$

The thrust of each engine is determined by assuming that the total thrust required at the start of cruise is equal to the total drag of the aircraft. At the specific thrust of interest, the cruise air mass flow rate can therefore be calculated $(\dot{m}_{cr} = F_{N,cr}/\hat{F}_{N,cr})$.

As the fuel is continuously burnt, the weight of the aircraft decreases and hence less lift is required to keep the aircraft afloat. In order to reduce the lift produced, one should not reduce the speed of flight, otherwise the time required to fly a given distance would increase. The lift coefficient C_L is also usually held constant at the value that gives the highest L/D ratio for fuel economy and aircraft range. Therefore, the only course available to reduce the lift is to climb to higher altitudes where the air density ρ_a is lower. For a long-range aircraft, the weight of fuel at take-off is a large fraction (of the order of 40%) of the total weight of the aircraft, hence the change in the required lift may be significant. An aircraft, cruising say at M = 0.82, may start the cruise at an altitude of, say, 31,000 ft or higher and may climb to, say, 41,000 ft; this gain in altitude, for reasons of practical constraints and legislation, may not take place continuously but in steps (of say 4000 ft).

The engines need to supply adequate thrust at all phases of a normal flight as well as under emergency situations (such as the failure of an engine). For engines with high bypass ratios, it is found that if the engine is sized to meet the thrust requirement at the start of cruise, it can produce sufficient net thrust at normal take-off conditions. This is primarily because the ram drag $\dot{m}V_a$ at take-off speed (which is normally limited to 90 m/s to restrict the required length of runway and to prevent the tyres of the wheels from overheating due to friction on the runway surface) is significantly lower than that at cruise speed (typically 250 m/s), particularly so for engines with low specific thrust having large value of the air mass flow rate \dot{m} . Although the non-dimensional temperature ratio T_{04}/T_{02} does not change much between the take-off, top of climb and cruise conditions, the absolute value of TET is the highest at take-off condition (primarily because T_{02} is highest when the aircraft is close to the ground: at ISA condition, the difference between T_{02} at take-off and that at start of cruise may be something like 30 K for a modern aeroengine) which may be 200-300 K higher than the melting point of the turbine blade material. Civil aero-engines are however not allowed to continuously operate for more

than 5 min at the take-off condition of maximum TET, otherwise the engine life will be seriously reduced.

The design point, from the point of view of the minimum fuel consumption, should correspond to the cruise condition. However, at the top of climb, the engine will need to produce the thrust required for cruise at the design altitude plus an additional amount required to impart a certain rate of climb to the aircraft. The aircraft forward speed is approximately 250 m/s and a typical rate of climb is 1.5 m/s. Thus, it is seen that, at cruise altitude, the aircraft climb angle θ to the horizontal is small $[\theta \sim \tan^{-1}(1.5/250) =$ 0.006 rad]. The net thrust may then be expressed by the relation: $F_{N,\text{top of climb}} = m_{aircraft}g(1/(L/D) + \sin\theta)$. For a well-designed modern subsonic aircraft, a typical value of L/D may be 20, so 1/(L/D) is 0.05, and, a typical value of sin θ may be 0.006. Hence, the thrust required at top of climb may be approximately 10–12% greater than that at level cruise. The design value of the limiting thrust is therefore usually set at top of climb condition. The non-dimensional parameters such as T_{04}/T_{02} , OPR and non-dimensional rotational speed of the HP shaft have the highest value at the top of climb condition.

Now, consider emergency situations such as the failure of one of the engines. Failure of an engine during take-off can lead to a dangerous situation, and the design requirement is that the aircraft would still be able to take-off and fly. For four-engine and three-engine aircrafts, the failure of an engine during take-off can be accommodated without any special measure, if the engine has been sized for the normal cruise condition. For a twin-engine aircraft, consideration of the failure of an engine during take-off needs special measure: the wing area is increased (that reduces the take-off speed) and the cruise altitude is increased. These measures ensure that the engine operates near its optimal design point at cruise and produce the necessary thrust at take-off should one of the two engines fail during take-off.

If the failure of an engine takes place during cruise, the cruise altitude is decreased to a value such that the thrust produced by the remaining engines becomes sufficient. A descent increases the thrust of the remaining engines primarily due to higher density of air ρ_a at a lower altitude, but this increases T_{02} . At the same nondimensional T_{04}/T_{02} , TET would therefore increase (compared to normal cruise condition) with some effect on the engine life (but this effect is not catastrophic since TET would still be a lot lower than the takeoff value). As a result of flying at the lower altitude, the aircraft range also decreases. The magnitudes of reduction in cruise altitude and aircraft range (due to the failure of one engine during cruise) increase as the number of engines (4, 3 or 2) decreases. For a twinengine aircraft, the necessary reduction in altitude may be such that the aircraft may not clear all mountains, and careful planning of the route may be necessary.

Fan diameter

The value of the fan diameter (Θ_{fan}) is a very important design parameter, because this is used in the scaling process for estimating the engine length, engine mass, nacelle diameter, and therefore the clearance between the nacelle and the lower surface of the wing, as well as that between the base of the nacelle and the ground. The fan diameter of each engine is calculated by the application of gas dynamic equations, considering the cruise atmospheric conditions, fan entry Mach number and the mass flow rate of air required for the engines to operate at the cruise specific thrust of interest. 18 Once Θ_{fan} is known, functional relationships given in the study of Jenkinson et al.²⁶ are used to determine all engine dimensions of the nacelle. Dimensions of the pylon and relations for positioning the engine are obtained from Airbus UK.33 Further details are given in Appendix 4.

Mass of engine and nacelle

Comprehensive in-service engine data⁵ for 30 turbofan engines of a number of major manufacturers (Rolls Royce, General Electric, Pratt & Whitney and CFM International) has been utilised in this study to establish empirical relationships between fan diameter and engine length. This enables the estimation of the bare engine length of new engines modelled within this parametric study. Further regression analysis (Appendix 5) has been used here to determine the mass of the new engines, using manufacturers' data for bare engine length, mass and fan diameter. The modelled nacelle mass is then calculated using an elaborate empirical expression described by Raymer.29 As the input variables, Raymer's formula uses length, diameter and wetted area of the nacelle, the engine mass, and various factors depending on the aircraft configuration. Further details are given in Appendix 5.

Fuel weight and fuel cost

The weight of fuel is an important factor. For a long-range flight of a large aircraft (e.g. Boeing 747-400, Airbus A340), the maximum weight of fuel may be about 45% of the maximum take-off weight (MTOW). In a typical mission, not all the fuel onboard is consumed during flight; a certain amount of reserves must be maintained. Hence, the total fuel weight consists of mission and reserve fuels. Mission fuel includes the fuel required for (a) take-off, acceleration and climb

to cruise altitude, (b) cruising flight, (c) descent, approach and landing and (d) manoeuvring. The reserve fuel includes fuel required for (a) diversion flight for a specified distance, including that for a missed approach and overshot manoeuvre, (b) hold for a specified duration at a specified altitude, (c) an extended duration of the flight and (d) contingency (a certain percentage of the block fuel). The reserve fuel depends on government legislations, operator policy and the type of flight (domestic or international). For this study, the amounts of fuel required to fly the typical and maximum missions for each aircraft are calculated using a method given by Torenbeek.²⁸ Mission fuel weight for typical range plus reserves, and, mission fuel weight for the design range are both calculated. The latter is usually greater and this is used to calculate MTOW.

For determining the fuel cost component of EDOC, the mass of the fuel actually consumed to complete the typical range (which is known as the block fuel, i.e. mission fuel plus fuel required for taxiing) is determined by the method of Torenbeek.²⁸ Torenbeek's method gives fuel mass per flight. The fuel cost component of EDOC (per engine per year) is calculated from the formula: fuel mass consumed per flight × price of fuel per unit mass × utilisation (flight/year)/number of engines.

Rubber aircraft sizing

The wing area of the rubber aircraft is sized by equating lift at the start of cruise to 97% MTOW and by assuming the wing to have a lift coefficient of 0.5, as suggested by Rossow et al.³⁴ The wing span, root chord, mean aerodynamic chord (MAC), spanwise engine location, horizontal tail area and vertical tail area are all sized from the wing area, based upon regression analysis of aircraft data from the studies of Jackson⁶ and Jenkinson et al.²⁶ covering a large number of aircrafts of several international manufacturers (e.g. Airbus, Boeing, McDonell Douglas). The fuselage length and width are sized from relations derived from existing aircraft data regarding the passenger capacity of the aircraft and the number of passengers seated abreast in a 2-class configuration. Appendix 5 outlines the empirical relations derived from the present regression analysis.

It should be noted that there may be constraints on the wing area arising from low speed requirements such as take-off distance and take-off speed. (It has been previously explained why the take-off speed is normally limited to $90 \, \text{m/s.}$) Stalling of the aircraft near the ground must be avoided; so, the lift coefficient at take-off (a typical value of $C_{L,\text{take-off}}$ may be 1.6) should be far away from the stalling value. The wing therefore may have to be sized to meet such constraints

at take-off. Additional constraints on aircraft size may arise from airport facilities. For example, major airports provide a standard $80 \times 80 \,\mathrm{m}^2$ bay area for each aircraft limiting both its wing span and length—this restriction on maximum wing span compelled Airbus to adopt a lower aspect ratio (thereby increasing induced drag) for their new large aircraft A380 compared to their usual design philosophy. The maximum length of the landing gear and the maximum diameter of the fan that can be hung underneath the wing may be constrained by ground handling facilities at existing airports constraining the maximum height of the fuse-lage above the ground. Practical constraints like these have not been implemented in the example calculations given in this article.

Rubber aircraft mass

Based on the historical data obtained from the study of Jackson, 6 the airframe mass of the rubber aircraft is determined here by formulating an empirical relationship for the airframe mass with the wing area, the design range under consideration and the number of passengers the aircraft would have capacity for in a 2class configuration (Appendix 5). We have shown later (Appendix 4) that the interference drag between the nacelle and the wing should be minimised for each rubber aircraft to obtain the minimum EDOC. This means that the landing gear length must be altered in order to maintain a suitable level of clearance between the base of the nacelle and the ground. This results in a change in gear mass which has been calculated in this study by developing a new empirical equation for the equivalent density of the gear as a function of the aircraft MTOW. The equation combines the methods of estimation for gear mass given in the studies of Raymer²⁹ and Roskam,³⁵ and data for real airframes given in Jenkinson et al.²⁶ The change in airframe mass due to the gear is calculated by multiplying the equivalent density of the gear and the change in gear length. The MTOW is ascertained by calculating the sum of the airframe weight, engine weight, fuel weight required for the design range and the payload.

Noise

In order that any selected specific thrust for a new engine is viable, the noise levels of the aircraft to which the engine is attached must be lower than the Stage 4 noise standards as set out by the ICAO. The ICAO Noise Certification Database³⁶ presents data on the effective perceived noise in decibels of the aircraft during takeoff, flyover and approach. A regression analysis has been performed linking the aircraft noise to engine sea level static thrust, sea level bypass ratio

and MTOW, allowing the estimation of the noise levels of each aircraft with various engines studied. The maximum specific thrust allowed by the noise consideration is shown on the graphs given in section 'Results and discussion'.

Emissions

As a preliminary indication of environmental suitability, the NO_x emissions index of the engines studied are estimated using GasTurb.¹⁷ Data regarding the emissions of real life engines can be found in the ICAO Engine emissions databank.³⁷ An approximate minimum specific thrust allowed by the emission legislation is calculated as a design check to make sure that the optimum specific thrust is within the correct boundaries. A recent publication³⁸ discusses various NO_x prediction methods that are available, and develops a new generic method that is simple and uses only publicly available information.

Thermodynamic optimisation of engine parameters

Thermodynamic optimisation scheme

According to Guha,⁸ concurrent optimisation of the main parameters is needed to exploit the full benefits of the thermodynamic cycle selected for any engine. It is clearly evident from equation (8) that the overall efficiency (η_o) governs the fuel economy for a given aircraft speed

$$\eta_o = \frac{V_a}{Q_{CV} \text{sfc}} \tag{8}$$

Therefore, it is the overall efficiency that is to be maximised (instead of the usual dealing with thermal and propulsive efficiencies separately).

In the optimisation method of Guha,⁸ the specific thrust is taken as a basic design parameter for the reasons cited in section 'Introduction'. The thermodynamic optimisation is thus carried out by concurrently finding a combination of FPR, overall pressure ratio (OPR), bypass ratio (B) and TET which maximises η_o (or minimises sfc) subject to the constraint that the specific thrust is kept fixed at a predetermined level. The value of the specific thrust at which the optimisation is performed is determined by an economic analysis (EDOC) that is the subject-matter of this article. The performance and optimisation of gas turbines with real gas effects are given in the study of Guha. ^{10,12}

The above thermodynamic optimisation method is very different from the usually employed parametric studies which involve the numerical calculation of engine performance as a single parameter is varied each time, while keeping all other parameters fixed—therefore not at their optimum values. Parametric studies with a single variable are inadequate in finding true optimum conditions in jet engine design (even if they produce the typical 'U-shaped' curves). Moreover, such parametric studies may be associated with large excursions in the value of the specific thrust which is not acceptable for real design. (In Figure 1, it has been shown from a careful compilation of the existing engine data that the values of cruise specific thrust of modern engines lie within a very narrow range.) The thermodynamic optimisation scheme of Guha,8 in contrast to previous studies, is also able to establish true thermodynamic optimums for the bypass ratio and TET, as discussed below.

The thermodynamic optimisation scheme⁸ shows the following.

- 1. For each value of the specific thrust, there is a bypass ratio that gives the minimum sfc. This is the optimum bypass ratio.
- The optimum bypass ratio increases with decreasing values of specific thrust. It depends only weakly on OPR
- 3. The value of TET corresponding to the optimum bypass ratio represents the optimum TET. (The value of TET obtained by this method would be different from that determined from consideration of thermal efficiency of the core engine alone.)
- 4. At low specific thrust level, the sfc versus *B* curves are sufficiently flat near the optimum value. One can therefore use significantly lower value of *B* than optimum, without appreciably increasing the sfc. This results in the use of lower TET, which allows the thrust growth potential of the engine in the future with the minimum change. A lower bypass ratio reduces the number of LP turbine stages and may avoid the use of a gear drive.
- 5. The sfc versus *B* curves for various specific thrusts cross each other indicating that there is an optimum specific thrust if bypass ratio were kept fixed at a particular value. This complex topic has been discussed in detail in the study of Guha;⁸ it has been shown in the study of Guha⁸ that optimising bypass ratio at fixed values of specific thrust produces different optimisation results from those obtained by optimising specific thrust at fixed bypass ratios. It has been further demonstrated in the study of Guha⁸ that the actual data of existing engines fall somewhere in between the two optimisation results.

The existence of the optimum bypass ratio and the optimum TET can be explained as follows: $\eta_o = \eta_D \eta_T$,

where $\eta_{\rm p}$ is constant at a fixed specific thrust; so, $\eta_{\rm o} \propto \eta_{\rm T}$. However, in the breakdown $\eta_{\rm o} = \eta_{\rm P}\eta_{\rm T}$, the thermal efficiency, $\eta_{\rm T}$, of a turbofan engine does not just depend on OPR, $T_{\rm 04}$ and component efficiencies, as it does in a ground-based gas turbine. It also depends on the dissipation of mechanical energy in its transfer from the core to the bypass stream. One may write

$$\eta_{\rm T} = \eta_{\rm core} F(B, \eta_{\rm KE}, \hat{F}_{\rm N}) \tag{9}$$

where η_{KE} is the efficiency of energy transfer from the core to the bypass stream and can be determined from the product of isentropic efficiencies of the fan, low turbine and bypass $(\eta_{\rm KE} \approx \eta_f \eta_{LPT} \eta_{bypass\ nozzle})$. The function F in equation (9) has been comprehensively computed in the study of Guha. The important properties of the function F are that it has a value of 1 when B = 0, and it decreases with increasing B. The function F asymptotically tends to η_{KE} for very large values of the bypass ratio: Lt $F \to \eta_{KE}$. With increasing bypass ratio, a higher \overrightarrow{prop} ortion of total energy is transferred to the bypass stream and thus the effect of the transmission loss becomes more important.

At fixed \hat{F}_N and OPR, an increase in B is accompanied by an increase in T_{04} , which raises η_{core} . This raises η_T initially. However, after the optimum value, any further increase in B makes η_T to decrease for two reasons.

- 1. As *B* increases, the reduction in the value of function *F* counteracts the gain in η_{core} .
- 2. Above a certain T_{04} , $\eta_{\rm core}$ itself starts decreasing due to real gas effects. (This important effect has been first discovered and explained by Guha. This happens in ground-based gas turbines as well as in aero gas turbine engines. Thus, the usual maxim that 'higher the temperature, higher is the efficiency' is not always valid.)

Application of the thermodynamic optimisation in this study

The new engine is optimised, following the optimisation principles explained above and with the help of the software GasTurb 10, for each value of specific thrust investigated. A number of mission dependent variables are input into GasTurb including: cruising altitude, Mach number, overboard bleed, power off-take and corrected inlet air mass flow for each mission.

An OPR of 50 is used. The burner exit temperature, FPR and bypass ratio are iterated to minimise sfc, with the constraint that the specific thrust is held constant at the chosen value. Nozzle guide vane cooling air and high pressure turbine cooling air ratios are each

varied between 0% and 10% in order to ensure the blade temperatures do not exceed 1200 K during cruise.

For each specific thrust investigated, the thermodynamic optimisation process is carried out under cruise conditions; GasTurb is then used to do further off-design calculations to find sea-level static conditions. In this way, GasTurb outputs the optimum bypass ratio and sfc at cruise, and sea level static thrust, which are utilised in order to obtain EDOC.

Guha^{8,9} has derived a number of explicit analytical relations specifying the optimum values of various parameters. These relations have been used here to compute initial guess for these variables; this ensures rapid convergence of the numerical optimisation performed by GasTurb. A few of these equations are given below for ready reference. The optimum FPR for separate stream as well as mixed stream turbofan engines are given in the study of Guha⁹

$$(FPR)_{\text{op,separate}}^{\frac{\gamma-1}{\gamma}}$$

$$= 1 + \frac{(\gamma - 1)}{2 + (\gamma - 1)M^{2}}$$

$$\times \left[\frac{(1+B)^{2}}{(B+1/\eta_{\text{KE}})^{2}} \left\{ \frac{\hat{F}_{\text{N}}}{\sqrt{\gamma R T_{\text{a}}}} + M \right\}^{2} - M^{2} \right]$$

$$FPR_{\text{op,mixed}}^{\frac{\gamma_{\text{g}}-1}{\gamma_{\text{g}}}} \left(\frac{BT_{02}}{\eta_{\text{f}}} + \frac{(c_{\text{pg}}/c_{\text{p}})\eta_{\text{t}}T_{04}}{OPR^{\frac{\gamma_{\text{g}}-1}{\gamma_{\text{g}}}}} \right)$$

$$= (c_{\text{pg}}/c_{\text{p}})\eta_{\text{t}}T_{04} - \frac{1}{\eta_{\text{c}}}T_{02}\left(OPR^{\frac{\gamma-1}{\gamma}} - 1\right) + \frac{BT_{02}}{\eta_{\text{f}}}$$
(11)

These equations compare well to numerically optimised FPR determined by GasTurb.

Guha⁸ formulated a method for calculating the optimum TET for a separate stream engine

$$\frac{T'_{04}}{T_{a}} \left[1 - (OPR)^{\frac{1-\gamma}{\gamma}} \right] \eta_{t}$$

$$= \frac{\gamma - 1}{2} (1 + B) \left[\eta_{t} \left\{ \frac{\hat{F}_{N}}{\sqrt{\gamma R T_{a}}} + M \right\}^{2} - \eta_{c} M^{2} \right] + \frac{1}{\eta_{c}} \left[(OPR)^{\frac{\gamma - 1}{\gamma}} - 1 \right] \tag{12}$$

where the introduction of an empirical correction shown in equation (13) gives near-perfect correlation with numerically optimised results from GasTurb

$$T_{04} = T'_{04} + 5[100/\hat{F}_{N,(lb/lb/s)} - B]$$
 (13)

Equation (13) is utilised to provide an initial burner exit temperature for GasTurb optimisation.

It has been derived in the study of Guha⁸ that when optimum FPR is used, the ratio of the fully developed jet velocities of the bypass nozzle and core nozzle is given by

$$V_{j,bypass}/V_{j,core} = \eta_{KE} \approx \eta_{fan} \eta_{LPT} \eta_{bypass\ nozzle}$$
 (14)

FARE and **RARE** computational models

The philosophy of the FARE model is to calculate, at each assumed specific thrust, the EDOC of an engine that is thermodynamically optimised and retrofitted to the chosen current aircraft that can perform a predefined mission. From many such calculations over a range of specific thrust values, the optimum specific thrust is determined that gives the minimum EDOC. The same procedure is then repeated for other mission profiles.

RARE model allows for, at each assumed specific thrust, the calculation of EDOC of an engine that is thermodynamically optimised in parallel with the optimisation of the dimensions of the airframe for a fixed-mission payload and range. From many such calculations over a range of specific thrust values, the optimum specific thrust is determined that gives the minimum EDOC. The same procedure is then repeated for other mission profiles.

It should be noted that the main purpose of this article is to establish the concept of optimum specific thrust and to develop a framework of calculations based on publicly available data that give reasonable values (in comparison to values for existing engines) of the optimum specific thrust. These objectives could be fulfilled by only developing the FARE model for which the design and optimisation methods given in this article are reasonably rigorous. We nevertheless have included a version of the RARE model as well to demonstrate that economic benefit can be obtained by optimising the aircraft and the engine together. The design and optimisation methods to be used in the RARE model are more complex and involved in nature. Some simplifications have been made to keep the target viable for this study. There may be scope for improvement here when the user has more resources available.

A few principal differences and similarities between the FARE and RARE models are summarised in Table 1.

In the FARE model, airframe dimensions, MTOW and typical range are fixed, design range is irreducible, and, the payload and fuel weight are variable. In the RARE model, payload, typical range and design range are fixed, and, airframe dimensions, fuel weight and MTOW are variable. The weight penalty is differently

Table 1. Comparison of FARE and RARE models.

	Parameter	FARE	RARE
Mission	Design range	Irreducible ^a	Fixed
	Typical range	Fixed	Fixed
	Payload	Variable ^b	Fixed
	Fuel weight	Variable	Variable
Aircraft	Dimensions	Fixed	Variable
	MTOW	Fixed	Variable
	OWE	Only engine weight component is variable	Variable ^c
	C_L	S_{wing} is fixed, C_L is calculated from equation (4)	$C_L = 0.5$ assumed, S_{wing} is calculated from equation (4)
Engine	Dimensions	Variable	Variable
	FF _i	Variable	1.0
	Spanwise location	Fixed	Variable

FARE: fixed aircraft rubber engine; RARE: rubber aircraft rubber engine; MTOW: maximum take-off weight; OWE: operating weight empty.

calculated in the two models. In both FARE and RARE models, the dimensions and weight of the engine are variable. For both models, the EDOC is calculated for a typical mission, and, the cruise Mach number and cruise altitude are fixed.

In the FARE model, the lift coefficient is calculated from equation (4): $C_L = (0.97 \mathrm{MTOW.}g)/(\frac{1}{2}\rho_a V_{TAS}^2 S_{wing})$. Since S_{wing} is fixed for a fixed aircraft, C_L is fixed for a constant altitude and aircraft speed. For the RARE model $C_L = 0.5$ is assumed, S_{wing} is therefore calculated. As previously explained, the purpose of the RARE study is to find the economic benefit of optimising the aircraft and the engine together. Rossow et al. suggest a value of 0.5 for the initial study of a generic transport aircraft configuration. Data given by Cumpsty also show that L/D is approximately maximum when $C_L = 0.5$. Thus, this value is chosen for the RARE model.

Another important difference between the FARE and RARE models is that, since changing the dimensions of the aircraft is permitted in the RARE model, the engine is positioned in the RARE model such that the interference drag between the wing and the nacelle is minimised. For this, the gully height is calculated such that the interference form factor becomes equal to unity $(FF_i=1)$. This may necessitate a change in the design of the landing gear to maintain necessary ground clearance.

Details of the FARE methodology

The following outlines the steps employed in the FARE methodology. A symbolic flow chart, where each

number corresponds to the numbered steps below, is provided in Figure 2 for clarity.

Step 1. Select a mission

Data^{6,7} of three baseline aircraft, the Boeing 737-600, 757-300 and 777-300ER, are used in this study as example aircraft that would typically operate over the three mission profiles, viz. short, medium and long ranges. Typical parameters for these missions are given in Table 2. (It should be noted that the three aircrafts are selected only as example applications of the COST models. The regression analysis, mentioned in section 'Determination of aircraft aerodynamic characteristics, dimensions and weight, and other design issues' and Appendix 5, takes into account a comprehensive data set for aircrafts of all major manufacturers.)

The number of passengers in 2-class configurations are 108, 239 and 370, respectively, for the three baseline aircrafts. The payload (i.e. number of passengers plus luggage) is variable in the FARE model. This determines the weight penalty described below. (The payload for the RARE model is fixed and the numbers of passengers for the three missions, in the RARE model, are maintained as that for the three corresponding baseline aircrafts.)

Step 2. Select an engine configuration

In order to maintain technological consistency, an engine configuration is chosen that suits well with the mission profile under consideration. Mixed stream engines are optimised for the short-range mission, while separate stream engines are optimised for the long-range mission. For the medium-range mission,

^aThe design range may increase but is not allowed to decrease.

^bVariation in payload taken into account in EDOC calculation as reduction in available seat kilometres.

^cVariation in mass of engine and landing gear alters OWE. An aircraft cost penalty is then applied to the EDOC calculation in relation to this mass increase. A negative penalty means a decrease in cost.

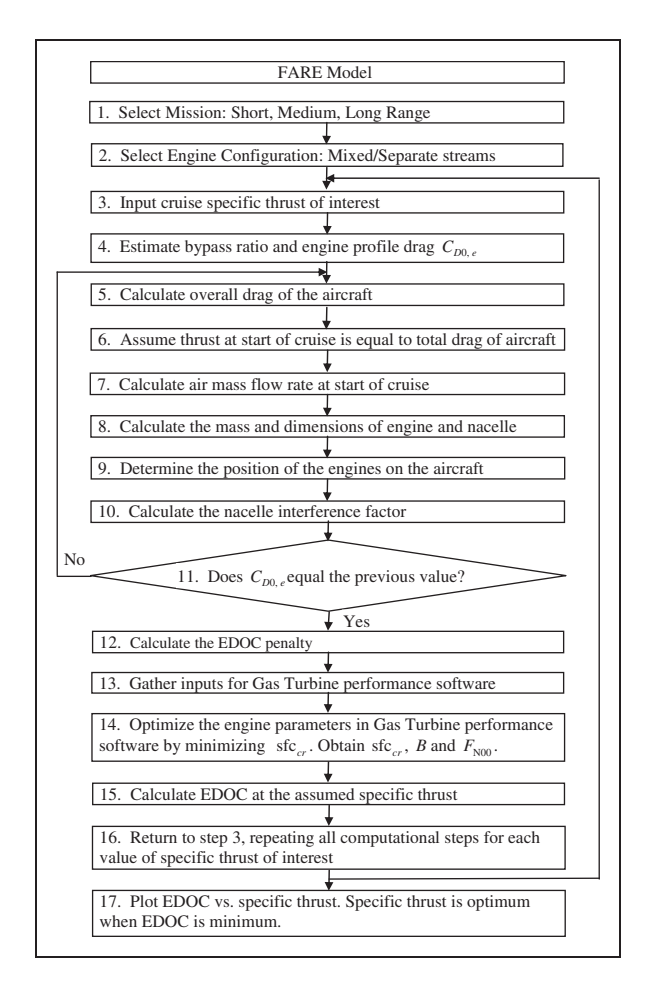


Figure 2. Flow chart for the FARE model.

Table 2. Parameters for study missions.

	Short range	Medium range	Long range
Design range (Nmi)	3191	2925	7880
Typical mission length (Nmi)	500	2000	5000
Cruise Mach number	8.0	0.82	0.84
Cruise altitude (ft)	35,000	35,000	35,000

both separate and mixed stream engines are optimised in order to determine the configuration which offers the lowest EDOC. The engines may have long or short cowl.

Step 3. Input cruise specific thrust of interest

A value for the cruise specific thrust range is selected at this stage of the computation within a typical range as exemplified in Figure 1. Steps 4–16 are repeated for each value of specific thrust of interest.

Step 4. Estimate bypass ratio and engine profile drag Guha⁸ outlines a trend between bypass ratio and specific thrust, and this trend is used to provide the initial guess for the bypass ratio. This is required as an initial input to the GasTurb calculations, and also for calculation of wetted area of the separate stream nacelle.26 An initial estimate for engine profile drag is required in order to help provide a sensible initial drag force on the aircraft at the start of cruise. An iterative procedure is used to achieve convergence on the engine dimensions and the engine profile drag.

Step 5. Calculate the overall drag of the aircraft The methods for calculating the induced and total drag are given in section 'Determination of aircraft aerodynamic characteristics, dimensions and weight, and other design issues' and Appendices 3 and 4.

Step 6. Calculate thrust at start of cruise $(F_{N,cr})$ It is assumed that the thrust at the start of cruise is equal to the total aircraft drag. The engines are optimised at the start of cruise, assuming that the aircraft has taken off at its MTOW and expended 3% of its MTOW in the climb.

Step 7. Calculate air mass flow rate at start of cruise (\dot{m}_{cr})

Once the required thrust at start of cruise is determined, the air mass flow rate can then be calculated, as the specific thrust is known for each set of calculations.

Step 8. Calculate the engine and nacelle mass and dimensions

Section 'Determination of aircraft aerodynamic characteristics, dimensions and weight, and other design issues' outlines the qualitative steps in the calculation of engine fan diameter. The bare engine dimensions and mass as well as the nacelle dimensions and mass are estimated as previously described.

Step 9. Determine the position of the engines on the wing In order to minimise the alterations to the current aircraft, the optimised engines are located at the same wing spanwise location as the current engines. Alterations in the mass and diameter of the engines would however, necessitate extensive structural analysis and possible redesign of the wing and pylon attachment region. The cost of such analysis/redesign is not considered within the EDOC calculation.

The chordwise location of the engine is set such that the front face of the nacelle, for all engines, is at the same chordwise position as the original engines utilised on each of the respective study aircraft. This is done to minimise the effect of the new engines on factors such as aircraft centre of gravity, stability and control, emergency egress, etc.

The vertical displacement of the engine is set such that the clearance height between the base of the nacelle and ground is kept constant for all engines. This height is based on that of the original engines installed on each of the respective aircraft. This placement ensures original criteria such as clearance in the event of a nose gear collapse are still met.

Step 10. Calculate the nacelle interference factor

The vertical position of the base of the nacelle under consideration is consistent with that of the current engine fitted to the study airframe, as explained in Step 9. Thus any increase in the nacelle diameter results in reduced clearance between the top of the nacelle and the underside of the wing. This leads to an increase in aerodynamic interference between the wing and the nacelle/pylon structure, which is included in the nacelle and pylon profile drag calculations.

Step 11. Iterate until the calculated engine profile drag equals the estimated value

Engine profile drag is determined as in section 'Determination of aircraft aerodynamic characteristics, dimensions and weight, and other design issues'. Any difference between this newly calculated value of engine profile drag and the previous estimation will result in a new total thrust requirement. This necessitates a new engine air mass flow rate and engine dimensions. Steps 5–11 are iterated until the value of engine profile drag converges.

Step 12. Calculate the EDOC weight penalty

Weight is a premium quantity in aviation, so the present authors felt that there should be a direct cost attribute of the weight in the mathematical model, so that heavier designs are automatically discouraged (unless there are other compensating attributes of the design). Note that the adopted mathematical model automatically captures the impact of engine size: a larger size of the engine gives rise to a larger amount of drag, this increases the engine thrust requirement, the value factor of the engine (VF, see section 'Determination of engine direct operating cost') and the engine price increase with increasing cruise thrust. Thus, there is a direct cost attribute of the size of the engine in the mathematical model. The authors wanted a similar cost attribute of the engine weight.

For the FARE model, the airframe (including its weight) and MTOW are fixed. The weights of the engine and the fuel are however altered as a result of the new design. We set our goal that the aircraft performance would not be compromised in any way because of the retrofitted engine: the aircraft–engine

combination would still be able to complete the typical mission with reserve fuel (section 'Determination of aircraft aerodynamic characteristics, dimensions and weight, and other design issues') as well as the design range (like the original or baseline aircraft, Table 2). Hence, in some cases, the payload may have to be altered to make sure that MTOW is not exceeded. For the purpose of this study, this payload reduction has been translated to a reduction in the number of passenger seats available. [According to Federal Aviation Administration, the average mass of a passenger is 190 lbm, and a typical baggage allowance is 23 kg per passenger; hence, the average payload mass per passenger may be taken as 109.2 kg. This may be used in the calculation of the reduction in the number of passengers.] This passenger reduction corresponds to a reduction in the aircraft available seat miles for the predetermined mission. A detailed analysis of typical airline airfares for the three study mission ranges has been performed in this study to calculate the potential revenue loss as a consequence of operating services with the new engines. This revenue loss is used as the EDOC weight penalty.

The way EDOC weight penalty is applied in the FARE model, there is only the possibility of (positive) penalty, no scope for negative penalty or gain. This is because the airframe and the seating arrangement are fixed in FARE model, so the number of passengers can be reduced from its design maximum, but cannot be increased. The design range would rather then increase. This is why we mentioned in Table 1 that the design range, for the FARE model, is 'irreducible'.

A particular model for the calculation of EDOC weight penalty has been devised here for numerical illustration. Calculations given later (section 'Results and discussion') show that, for the values of specific thrusts considered, the EDOC weight penalty does not arise for medium- and long-range missions and applies only at the low end of specific thrusts for short-range missions (i.e. the EDOC weight penalty does not affect the optimum value of specific thrust even for the short-range mission). The fundamental concepts developed in this study or the major conclusions do not alter as a result of the EDOC weight penalty. Readers or users of this article may apply any other, more suitable, weight penalty model, as they think fit.

Step 13. Gather inputs for analysis by gas turbine performance software

Estimated values of *B*, FPR, T_{04} , etc. are required for initialising computation by GasTurb, as detailed in section 'Thermodynamic optimisation of engine parameters'. Power off-take, overboard bleed, ratio of total pressure across the inlet, corrected mass flow rate at inlet, isentropic efficiencies of components, etc. are specified.

Step 14. Optimise the engine in a gas turbine performance software

Each engine is optimised in a gas turbine performance software such as GasTurb to provide a minimum sfc solution. The details of this process are outlined in section 'Thermodynamic optimisation of engine parameters'. The output of the computation gives sfc_{cr} , B and F_{N00} which are required in the calculation of EDOC.

Step 15. Calculate EDOC at the assumed specific thrust The total EDOCs are calculated as discussed in section 'Determination of engine direct operating cost', including the EDOC penalty defined in Step 12. The prices of the engine and the nacelle depend on $F_{N,cr}$ and sfc_{cr} . The fuel cost depends on sfc_{cr} . The maintenance cost depends on sfc_{cr} , B and F_{N00} .

Step 16. Repeat all computational steps for each specific thrust of interest

Steps 4–15 are repeated until an engine of each specific thrust of interest has been thermodynamically optimised, with the total EDOC of each of these engines calculated.

Step 17. Plot EDOC results for each mission studied Having ascertained the EDOCs of each GasTurb optimised engine, the optimum specific thrust is found for the engine with the minimum EDOC.

Details of the RARE methodology. A symbolic flow chart for the computational steps needed for the RARE model is given in Figure 3. A comparison of Figures 2 and 3 reveals the similarities and differences of the two models described at the beginning of this section. The computational details of the steps that are similar to FARE model can be seen in section 'Details of the FARE methodology'. The details about rubber aircraft mass and rubber aircraft sizing are given in section 'Determination of aircraft aerodynamic characteristics, dimensions and weight, and other design issues'. For brevity, these are not repeated here. However, a discussion on Step 18 of Figure 3 regarding how the EDOC penalty is calculated for the RARE model is given below. Note that the EDOC penalty in the FARE model (see Step 12 of section 'Details of the FARE methodology') is differently applied compared to that in the RARE model.

Step 18. Calculate change in airframe mass due to new engine and EDOC penalty

The airframe mass in RARE model is variable for two primary reasons. First, the mass of the landing gear changes with the change of an engine (Step 12 of Figure 3). Second, the airframe weight is correlated to the wing area (Appendix 5), which is altered to provide sufficient lift to complete each mission. Since the payload mass and design range are fixed, there is a requirement for an operating cost penalty or reward for any alteration in airframe weight due to changes in engine dimensions and mass

 Δ airframe mass)_{RARE,optimised engine} $-(airframe mass)_{RARE,baseline engine}$ (15)

Equation (15) gives the change in airframe mass directly attributable to the new engine. (Note that we have not used the changes of the airframe mass from the baseline airframe mass. Instead, it is the mass difference in two optimised airframes, one with the baseline engine and the other with the optimised engine.) Using Boeing aircraft pricing data, ³⁹ an empirical equation is derived for the relationship between airframe price and mass. Thus, the alteration in airframe mass can be correlated to a change in airframe price and as this is directly attributable to the new engine design, it may be incorporated as a penalty in the EDOC calculation.

In devising the above weight penalty model, we have applied the following philosophy. Weight is a premium quantity in aviation: there should be a cost attribute (penalty) if the aircraft–engine combination becomes heavier than the baseline design; there should be a cost attribute (reward or negative penalty) if the aircraftengine combination becomes lighter than the baseline design. In the RARE model, the mission range and payload are kept fixed at their baseline values. The purpose of the RARE model is to extract additional benefit by optimising the engine and the aircraft together. It is true that any reduction of weight would be reflected in the reduced price of the airframe-engine combination. If we were calculating the DOC of the aircraft, then this adjustment would be in-built in the mathematical model. But we are determining EDOC and the optimum specific thrust of the engine. We have therefore tried to determine the change in airframe mass directly attributable to the new engine and have used the corresponding change in airframe price as the penalty or reward (negative penalty) in EDOC. It may be asked who would actually pay any 'reward' to the engine manufacturer? This question is somewhat similar to that of who would actually reap the benefit of reduced interference drag between the engine and the fuselage. The engine manufacturers often quote sfc for the uninstalled engine, though the installed sfc would be higher on account of

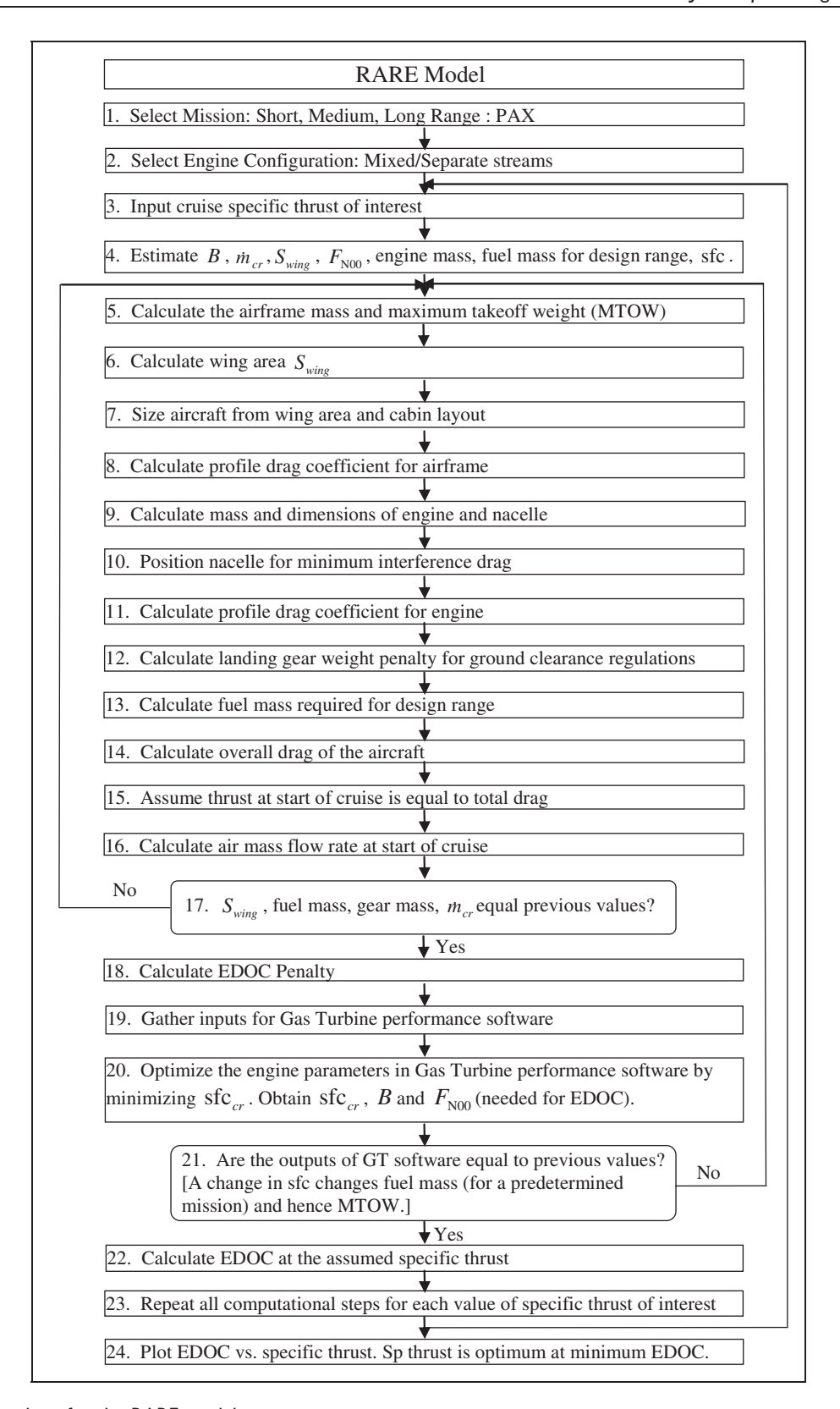


Figure 3. Flow chart for the RARE model.

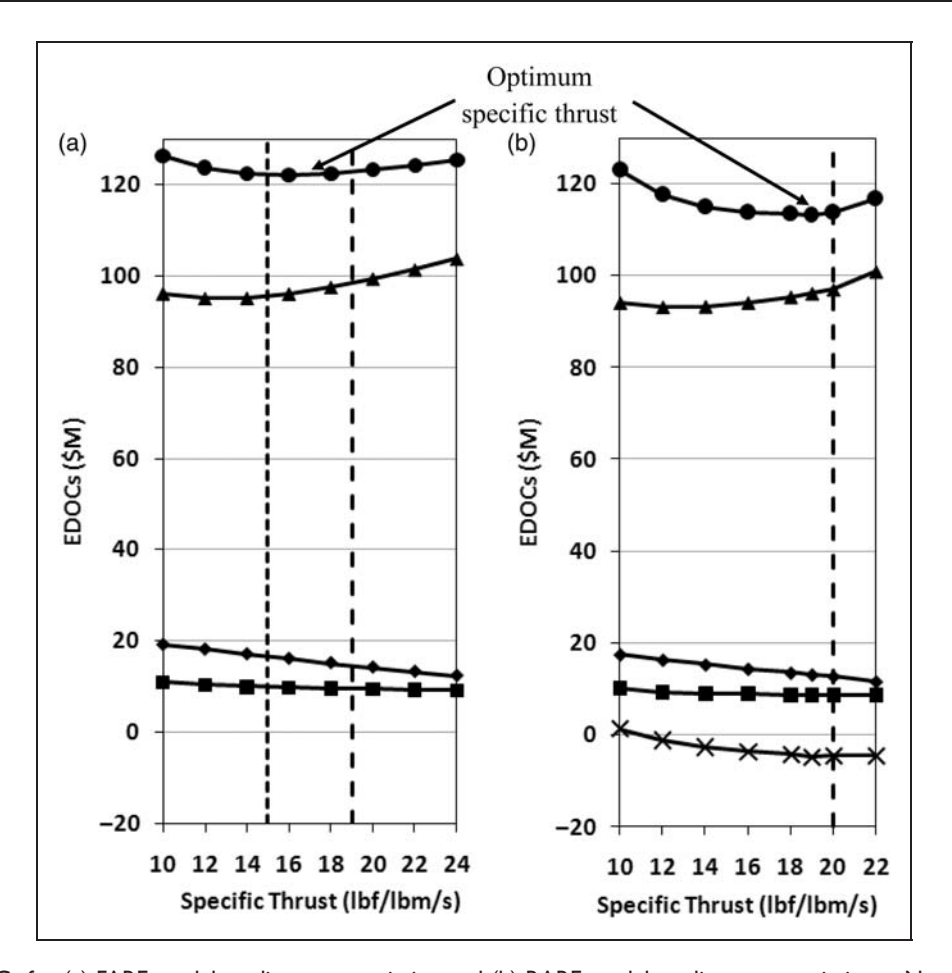


Figure 4. EDOCs for (a) FARE model medium-range mission and (b) RARE model medium-range mission. Note: → total cost, → fuel cost, → engine price, → maintenance cost, → weight penalty, · · · spatial limit and - · noise limit.

drag on the nacelle and interference drag; it may not be clear to whose budget this difference in sfc should be charged to. Even within the same engine company, there may be tension between two departments (such as the compressor and the turbine departments) on the book-keeping of loss particularly in non-uniform flow, and depending on the particular practice the quoted values of the isentropic efficiencies of the components may be slightly different. We have therefore taken a holistic academic viewpoint in ascribing penalty or reward to the design of engines.

A particular model for the calculation of EDOC penalty has been devised for numerical illustrations of this article. The value of the optimum specific thrust slightly changes as a result of application of the penalty, but the concepts or major conclusions do not alter. Readers or users of this article may apply any other, more suitable, cost penalty model, as they think fit.

Results and discussion

Figure 4 shows illustrative calculations for the variation of EDOC and its components with varying specific

thrust for both FARE and RARE models. The EDOC curve shows a minima which defines the optimum value of the specific thrust. A comparison of the FARE and RARE model results shows that the minimum value of the RARE model is lower than the minimum value of the EDOC for the FARE model (by 7.5% in the example calculation). This shows that the optimisation of the airframe-engine combination is more cost-effective than that of the engine alone.

Figure 4 shows that the reduction in specific thrust results in increased engine price and maintenance costs. The variation in fuel mass with specific thrust is more complex. Decreasing specific thrust means an increase in propulsive efficiency. However, the thermal efficiency (and another factor related to transfer of energy from the hot stream to the bypass stream) needs subtle consideration, as shown in the study of Guha. Moreover, the mass of engine increases with decreasing specific thrust and this counteracts any reduction in fuel mass due to decreased sfc. A larger nacelle means greater wetted area and an increase in profile drag (in both FARE and RARE models) and also an increase in interference drag in the FARE model. The increase in

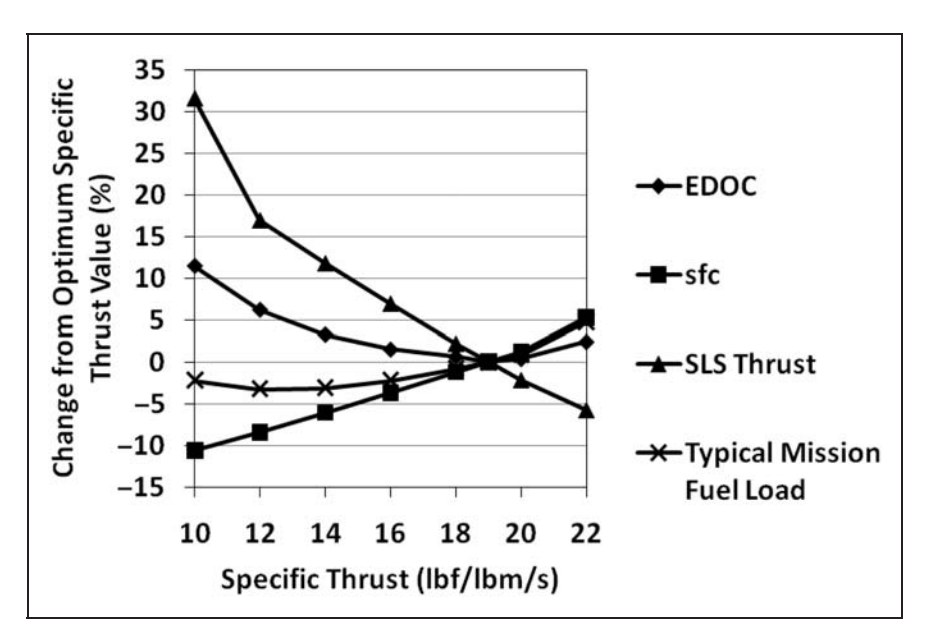


Figure 5. Effect of change in specific thrust on EDOCs, sfc, F_{N00} , and fuel mass for the FARE medium-range mission, altitude = 10,668 m, M = 0.82, OPR = 50, isentropic efficiencies = 0.9.

drag results in an increase in thrust required for straight and level flight at the design cruise Mach number.

In Figure 4, we only show the results for the medium-range mission for brevity. Such calculations are repeated for other lengths of mission and it is found that, as mission range is increased the total EDOCs increase due to increases in engine price, maintenance costs and fuel costs, but the optimum specific thrust decreases. This reduction in optimum specific thrust can be explained by the increasing proportion of fuel costs to total EDOCs, e.g. ranging from 69% for the FARE short-range mission to 83% for the FARE long-range mission over a 14-year study period (for a fixed fuel price of \$3/gallon). [Results of all three (short, medium, and long ranges) missions are given later in Figure 6. The proportions of three main components (viz. fuel costs, engine price and maintenance costs) of the EDOC are given in Figure 6 for each of three missions for a range of fuel price. Figure 6 also shows the variation of the optimum specific thrust for all three missions.]

In calculating the optimum specific thrust for the medium-range engines, both mixed and separate stream options had to be considered so as to determine the option resulting in the lowest EDOCs. The mixed stream engine produced 0.4% lower EDOCs over 14 years than the separate stream engine. This closeness implies that considerable analysis would be required before selecting the engine configuration in reality.

There may be three critical factors that limit the allowable specific thrusts: noise regulations (both FARE and RARE models), emission regulations

(both models), and the space available under the wing (FARE model). The noise regulation determines the maximum allowable specific thrust, while emissions and under-wing space requirements set the minimum. As the aircraft mass increases, the noise regulations become more stringent, resulting in a narrower window of allowable specific thrust. As the specific thrust decreases, the jet noise decreases and the contribution of the fan noise to the total noise becomes increasingly important. At very low values of the specific thrust, the fan noise may become the dominant source of engine noise. The fan noise is very sensitive to the fan tip speed which can be reduced by gearing, but the use of gearing would introduce other engineering difficulties and challenges. (For long-range missions, the simple models for emissions used in GasTurb produced a reasonable match with values of real engines,³⁷ but our calculations for medium-range missions did not. For this reason, the emission limiter is not shown in Figure 4. A recent publication³⁸ discusses various NO_x prediction methods that are available, and develops a new generic method that is simple and uses only publicly available information.)

The penalty (Step 12, section 'Details of the FARE methodology') calculated for the FARE short-range mission becomes sizeable at lower values of specific thrust. For example, at 10 lbf/lbm/s, the capacity of the 108-seat aircraft must be reduced by 14 passengers in order to operate at the design MTOW. This leads to a potential decrease in airline revenue of \$57.8 million over a 14-year period. This penalty reduces to zero as specific thrust increases to 14.0 lbf/lbm/s, and has no

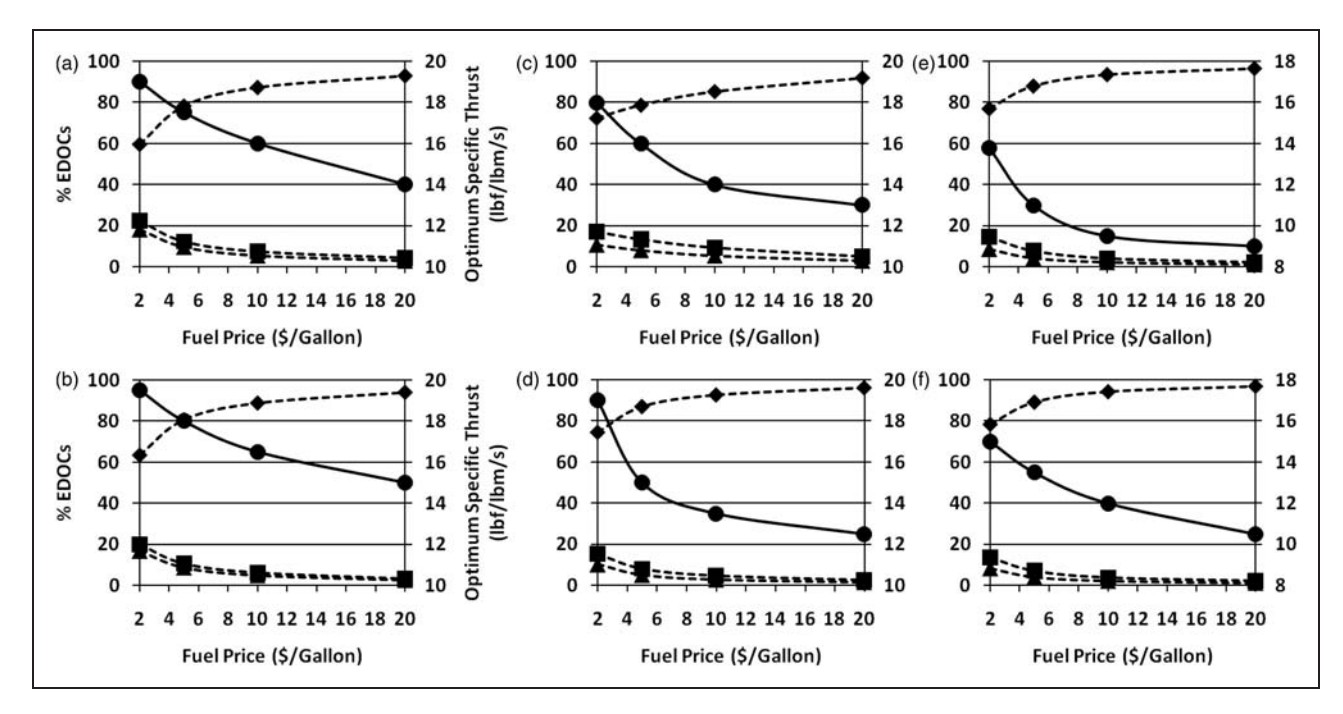


Figure 6. Effect of fuel price on optimum specific thrust and EDOC makeup for (a) short-range FARE with mixed stream engines, (b) short-range RARE with mixed stream engines, (c) medium-range FARE with mixed stream engines, (d) medium-range RARE with mixed stream engines, (e) long-range FARE with unmixed flow engines and (f) long-range RARE with unmixed flow engines. Note: ——optimum specific thrust, — fuel cost as % of EDOC, ——engine price as % of EDOC and —— maintenance cost as % of EDOC.

Table 3. Comparison of FARE and RARE optimised engine results for short-range missions with CFM 56-7B22.

Parameter	FARE-SR	RARE-SR	CFM 56-7B22	
Engine length (m)	2.05	2.03	2.51	
Θ_{fan} (m)	1.41	1.40	1.55	
Cruise bypass ratio	6.7	6.4	5.2	
Engine mass (kg)	1683	1817	2366	
Cruise sfc (g/kN.s)	14.9	15.6	14.9	
$\hat{F}_{N,cr}$ (lbf/lbm/s)	19.0	19.5	19.0	
EDOC (\$M)	57.3	57.0	_	

FARE: fixed aircraft rubber engine; RARE: rubber aircraft rubber engine; EDOC: engine direct operating cost.

effect on the calculation of the short-range optimum specific thrust, which is 19.0 lbf/lbm/s. For all specific thrusts investigated for the FARE medium-range mission, the combination of the mass of fuel required to complete the design mission and the mass of the thermodynamically optimised engines is lower than the sum of the mass of the maximum fuel load of the Boeing 757-300 and the mass of two RB211-535E4-B installed engines. Therefore, the FARE model penalty does not affect the EDOC for specific thrusts greater than or equal to 10 lbf/lbm/s. This can be seen in Tables 3 to 5 which provide a compilation of some key parameters

of the optimised engines from the current study (for a fixed fuel price of \$3/gallon) along with the parameters of the baseline engines used on the three respective aircraft. As in the case of the medium-range mission, no penalty arises for the long-range mission for the values of the specific thrust investigated.

As a part of the study, the RARE model airframe mass was compared to the airframe mass which would be encountered in the event that current engines were utilised on the aircraft.²⁴ Figure 4 shows that at low values of the specific thrust there may be a penalty due to the increase in engine mass (over the baseline

Parameter	FARE-MR	RARE-MR	RB211-535E4-B
Engine length (m)	2.92	2.68	3.00
Θ_{fan} (m)	1.89	1.76	1.88
Cruise bypass ratio	7.3	6.9	4.3
Engine mass (kg)	2928	2561	3295
Cruise sfc (g/kN.s)	14.8	15.3	17.5
$\hat{F}_{N,cr}$ (lbf/lbm/s)	18.0	19.0	19.0
EDOC (\$M)	122.5	113.3	_

Table 4. Comparison of FARE and RARE optimised engine results for medium-range missions with RB211-535E4-B.

FARE: fixed aircraft rubber engine; RARE: rubber aircraft rubber engine; EDOC: engine direct operating cost.

Table 5. Comparison of FARE and RARE optimised engine results for long-range missions with GE90-115B.

Parameter	FARE-LR	RARE-LR	GE90-115B
Engine length (m)	5.36	5.01	4.90
Θ_{fan} (m)	3.24	3.05	3.26
Cruise bypass ratio	10.4	9.6	8.4
Bare engine mass (kg)	7808	6985	7561
Cruise sfc (g/kN.s)	14.5	14.8	15.3
$\hat{F}_{N,cr}$ (lbf/lbm/s)	13.8	15.0	_
EDOC (\$M)	294.3	290.0	_

FARE: fixed aircraft rubber engine; RARE: rubber aircraft rubber engine; EDOC: engine direct operating cost.

engine). But as the specific thrust increases, the RARE optimisation process results in a gain (shown by negative values of the penalty).

The process of minimising sfc in GasTurb is performed by finding the optimum combination of bypass ratio, FPR, and TET for each engine studied. For all design missions investigated, the sfc of the optimised engine is greater for the RARE model than the FARE model, as shown in Tables 3 to 5. This can be attributed to the higher optimum specific thrusts of the RARE model engines than the FARE model engines, which have been increased by the presence of the (negative) RARE penalty. Although the sfc is higher, the minimum EDOC for RARE model is lower than the minimum EDOC of the FARE model showing the benefit of optimising the engine and airframe together.

For the RARE model, the effect of altering the interference factor between the wing and the nacelle has been investigated. Increasing the distance of separation between the nacelle and the wing results in an increase in gear length, therefore increasing airframe mass. This in turn, increases the drag, thereby increasing the thrust requirement. However, a reduction of the separation results in a reduction of the gear mass, but the interference drag between the nacelle and the wing is greatly increased. A study in the variation of EDOC and its various components as a function of the interference

drag factor was performed. It was found that the optimum location for the nacelle is that which minimises the interference drag and in turn the EDOC (this occurs when the value of interference form factor FF_i is 1.0, see Appendix 4).

Figure 5 shows the effects of change in specific thrust on EDOCs, sfc, $F_{\rm N00}$, and fuel mass for the FARE medium-range mission, as a percentage change in respective values from those at the optimum specific thrust (19 lbf/lbm/s). Figure 6 gives a parametric study in the variation of EDOC and its components with varying specific thrust for six cases (FARE and RARE versions for each of the three mission ranges). For the long-range mission, the optimum specific thrust reduces from 14 to 9 lbf/lbm/s for the FARE model when the fuel price is increased from \$2/Gallon to \$20/gallon. As there are currently no commercially available turbofans capable of providing this low specific thrust, these results suggest that radical changes in the engine design and its integration may be necessary.

The engines optimised for implementation on shortand medium-range missions do not show such dramatic alterations in optimum specific thrust with increasing fuel price, but as fuel price is increased to \$20/gallon, the fuel cost contribution exceeds 90% of the EDOCs in all cases. The optimum specific thrusts for mediumrange FARE and RARE models would then be 13 and

13.5 lbf/lbm/s, respectively, while the short-range FARE and RARE models would have optimum specific thrusts of 14 and 15 lbf/lbm/s, respectively.

Conclusion

A systematic methodology for the determination of optimum specific thrust of civil turbofan engines has been presented. The optimum specific thrust determined here complements the thermodynamic optimisation strategy for engine parameters developed in a previous publication by Guha. The process of optimisation thus involves a complex multidisciplinary methodology involving aerodynamics, thermodynamics, structures, system integration, economics, legislations, and other design and operational issues. With this aim, a user-friendly general-purpose computational tool has been developed with the acronym COST. Comprehensive data regarding existing aircraft and engines of all major manufacturers have been used in the database of COST which offers a flexible choice to the user about mission and configuration of the aircraft and engine.

This article has defined two models for turbofan optimisation: FARE and RARE models, both of which have been used to investigate a range of specific thrusts in order to determine the optimum specific thrust which minimises EDOC. Both models account for the effect that cruise drag and the nacelle and pylon drag have on the cruise thrust requirements of the engine. The models have been utilised in the calculation of optimum specific thrusts for engines fitted to airliners operating on typical short-, medium- and long-range missions. A wide variety of fuel prices have been considered in each case, and it has been demonstrated that the optimum value of specific thrust decreases with increasing fuel price. A comparison of the FARE and RARE model results shows that the minimum value of the RARE model is lower than the minimum value of the EDOC for the FARE model. This shows that the optimisation of the airframe-engine combination is more cost-effective than that of the engine alone. Present calculations show that, as mission range is increased, the total EDOCs increase due to increases in engine price, maintenance costs and fuel costs, but the optimum specific thrust decreases.

In calculating the optimum specific thrust for the medium-range engines, both mixed and separate stream options are considered so as to determine the option resulting in the lowest EDOCs. The mixed stream engine produced 0.4% lower EDOCs over 14 years than the separate stream engine. This closeness implies that considerable analysis would be required before selecting the engine configuration in reality.

The few engine cost studies that are available in the literature do not provide the details of calculation, and

depend on proprietary information. The presented methodology may be the only of its kind that attempts to determine the optimum specific thrust based on publicly available data and clean-sheet analysis. Moreover, a new, robust thermodynamic optimisation methodology of Guha⁸ has been integrated into the present cost study. A comparison of Figure 1 (actual data for existing engines) and Figure 6 (predictions of present methodology) shows that the optimum specific thrusts which are calculated by both FARE and RARE models are consistent with those estimated for a range of existing engines. Thus, one can see that the specific thrusts of engines currently utilised on airliners are well suited for current market conditions. The developed systematic method provides a rationale for the values of specific thrust found in existing engines and the basis for future designs.

For the short- and medium-range studies, when fuel price is raised to a substantially elevated price of \$20/gallon, the optimum specific thrust is between 13 and 15 lbf/lbm/s (which is at the lower end of current values, as seen in Figure 1) in all cases, showing that current turbofan technology may still be applicable in achieving minimum EDOC.

Should fuel prices continue to rise to the elevated prices examined here, it has been shown that for typical long-range missions, the optimum value of specific thrust could go as low as 9 lbf/lbm/s. At such low specific thrusts, geared turbofans or other low specific thrust configurations such as open rotor engines may be necessary. Considerable costs would be associated with the increased research, development and testing of this technology. Nevertheless, this may become imperative for airline operations should there be a very large increase in fuel price (as studied here) or with the introduction of more stringent noise and emissions regulations.

Funding

This research received no specific grant from any funding agency in the public, commercial, or not-for-profit sectors. Regular MEng Project formed the basis of the work.

Acknowledgements

The authors are grateful to NA Mitchell (an ex-employee of Rolls Royce Bristol), Askin Isikvaren and Airbus UK for running the Design Project at the Aerospace Engineering Department of University of Bristol. The authors are grateful to the reviewers of this manuscript for their detailed comments which have considerably improved the presentation of the material in this article. The authors thank the reviewers for recognising: 'This paper presents a complex multidisciplinary study of a civil transport airplane as a total system'; 'This study provides a systematic methodology to determine the optimum specific thrust for civil turbofan engines.' The present form of the paper is almost completely written by Abhijit Guha after he joined the Indian Institute of Technology Kharagpur as a professor.

References

- Bennett HW. Aero engine development for the future. Proc IMechE, Part A: J Power and Energy 1983; 197: 149–157.
- Jackson AJB. Some future trends in aero engine design for subsonic transport aircraft. *Trans ASME J Eng Power* 1976; 98: 281–289.
- 3. Wilde GL. Future large civil turbofans and powerplants. *Aeronaut J* 1978; 82: 281–299.
- Younghans JL, Donaldson RM, Wallace DR, et al. Preliminary design of low cost propulsion systems using next generation cost modelling techniques. ASME J Eng Gas Turb Power 1999; 121: 1–5.
- Rolls-Royce Aero Data. VCOM 5013, Issue 2, September 2002.
- 6. Jackson P. *Jane's all the world's aircraft 2005-2006*, 96th edn. Coulsdon: Jane's Information Group, 2005.
- Jenkinson L. Data A: aircraft data file. In: Civil jet aircraft design. New York, NY: Elsevier, 2009. Available at: http://www.elsevierdirect.com/companions/97803407415 28/appendices/data-a/default.htm (2009, accessed 8 April 2009).
- 8. Guha A. Optimisation of aero gas turbine engines. *Aeronaut J* 2001; 105(1049): 345–358.
- Guha A. Optimum fan pressure ratio for bypass engines with separate or mixed exhaust streams. AIAA J Propul Power 2001; 17(5): 1117–1122.
- Guha A. Performance and optimisation of gas turbines with real gas effects. *Proc IMechE*, *Part A: J Power and Energy* 2001; 215(4): 507–512.
- 11. Guha A. An efficient generic method for calculating the properties of combustion products. *Proc IMechE*, *Part A: J Power and Energy* 215(3): 375–387.
- Guha A. Effects of internal combustion and non-perfect gas properties on the optimum performance of gas turbines. *Proc IMechE, Part C: J Mechanical Engineering Science* 2003; 217(4): 1085–1099.
- IATA. Economics: jet fuel price development, Montreal, QC, Canada: International Air Transport Association. Available at: http://www.iata.org/whatwedo/economics/fuel_monitor/price_development.htm (2009, accessed 18 March 2009).
- 14. Robinson T. Money meltdown: winners and losers. *Aerospace Int*, November 2008, p.15.
- 15. Gardner R. How green is your contrail?. *Aerospace Int*, March 2009, pp.14–17.
- 16. Robinson T. Engines: prize flight. *Aerospace Int*, July 2008, pp.34–37.
- 17. Kurzke J. *GasTurb 10 user manual*. Germany: Joachim Kurzke, 2004.
- 18. Cumpsty N. *Jet propulsion*. Cambridge: Cambridge University, 1997.
- Rüd K and Lichtfuss HJ. Trends in aero-engine development, aspects of engine airframe integration for transport aircraft. In: *Proceedings of the DLR workshop*, Braunschweig, Germany, 6–7 March 1996, DLR Mitteilung 96-01.
- 20. Meece CE Gas turbine technologies of the future. In: Proceedings of the international symposium on

- airbreathing engines (ISOABE), Melbourne, Australia, 10–15 September 1995.
- 21. Birch NT. 2020 vision: the prospects for large civil aircraft propulsion. *Aeronaut J* 2000; 104(1038): 281–289.
- Cloft TG and Muldoon PL. Ultra High Bypass (UHB) engine critical component technology. ASME paper no. 89-GT-229. New York, NY: ASME, 1989.
- Definitions and inputs for range and direct operating cost calculation. Appendix 1, G(T) 5656. Brussels, Belgium: Association of European Airlines, 1990.
- 24. Boylan D and Gallagher P. Determination of optimum specific thrust. MEng report: project no. 1295, March 2009. Bristol: Department of Aerospace Engineering, University of Bristol.
- Abdul Rahman AZ and Hassan A. Determination of optimum specific thrust. MEng report: project no. 1031, March 2003. Bristol: Department of Aerospace Engineering, University of Bristol.
- 26. Jenkinson LR, Simpkin P and Rhodes D. *Civil jet aircraft design*. London: Arnold, 1999, pp.197–202.
- Roskam J. Appendix B: engine price data. In: Airplane design: airplane cost estimation: design, development, manufacturing and operating. Airplane design series VIII. Lawrence, KS: DAR Corporation, 2002, pp.321–324.
- 28. Torenbeek E. Cruise performance and range prediction reconsidered. *Prog Aerosp Sci* 1997; 33: 285–321.
- Raymer DP. Aircraft design: a conceptual approach, 3rd edn. Reston, VA: AIAA, AIAA Education Series, 1999.
- 30. Kroo I. *Aircraft design: synthesis and analysis course notes.* Stanford, CA: Stanford University, 2008. Available at: http://adg.stanford.edu/aa241 (accessed 8 February 2008).
- Sommer SC and Short BJ. Free-flight measurements of turbulent-boundary-layer skin friction in the presence of severe aerodynamic heating at Mach numbers from 2.8 to 7.0. NACA-TN-3391. Washington, DC: NASA, 1955.
- 32. Avallone EA, Baumeister T and Sadegh A. *Mark's stan-dard handbook for mechanical engineers*. 11th edn. New York, NY: McGraw-Hill, 10th Revised ed. New York, NY: McGraw-Hill, 1996, p.46.
- Airbus UK. AENG30001/M2003 aerospace vehicle design & system integration 3F/4F: aerodynamics. Bristol, UK: Aerospace Engineering Department, University of Bristol, 2007.
- 34. Rossow CC, Godard JL, Hoheisel H, et al. Investigation of propulsion integration interference effects on a transport aircraft configuration. *J Aircr* 1992; 31(5): 1022–1030.
- 35. Roskam J. *Airplane design part V: component weight esti- mation.* Ottawa, KS: Roskam Aviation and Engineering Corporation, 1989, pp.81–82.
- ICAO. Noise data bank, London: International Civil Aviation Organization, 2009. Available at: http:// noisedb.stac.aviation-civile.gouv.fr/find.php (accessed 12 March 2009).
- ICAO. Engine emissions databank, London: International Civil Aviation Organization, 2009. Available at: http://www.caa.co.uk/default.aspx?catid=702&pagetype=90 (accessed 12 March 2009).

38. Chandrasekaran N and Guha A. Study of prediction		Q_{CV}	calorific value of fuel
methods for NO_x emission from turbofan engines.		R	specific gas constant of air
AIAA J Propul Power 2012; 28(1): 170–180.		Re	Reynolds number
39. Boeing Commercial Airplanes. Boeing, 2009. Available		R_L	labour rate (\$/h)
at: http://www.boeing.com/commercial/prices (accessed		S	area
10 January 2009).		S_{wet}	wetted area
		$T^{"e}$	static temperature
		T_a	temperature of ambient air
Appen	Appendix I		total temperature
Notatio	Natation		TET
Notation		T_{04} V	flow velocity
A	cross-sectional area	V_a	aircraft velocity
AR	aspect ratio	V_{stall}	aircraft stall velocity
b	wing span	W	width
B	bypass ratio	x'	horizontal displacement from leading edge of
c_e	wing chord length at the location of engine		wing to P^*
c	attachment	x_e	longitudinal distance from aircraft nose to
c_p	specific heat of air at constant pressure	κ_e	leading face of nacelle
c_{pg}	specific heat of combustion gas at constant	v	longitudinal distance from aircraft nose to
epg	pressure	X_{w}	leading edge of wing root
c_r	wing chord length at the wing root		
C_D	total drag coefficient of the aircraft	y_e	spanwise engine displacement from the centre
CD	$(C_D = C_{D0} + C_{Di} + C_{DW})$		of the fuselage
C_{Di}	induced drag coefficient of the aircraft		in anti- and a factor of a factor
C_{Di} C_{DW}	wave drag coefficient	γ	isentropic index of air
	profile (zero-lift) drag coefficient of the	γ_g	isentropic index of combustion products
$C_{D0,a}$	- · · · · · · · · · · · · · · · · · · ·	η_c	isentropic efficiency of the compressor
C	airframe	η_{core}	thermal efficiency of the core engine
$C_{D0,e}$	profile (zero-lift) drag coefficient of the	η_f	isentropic efficiency of the fan
	engine (nacelle + pylon, including	$\eta_{ ext{KE}}$	efficiency of energy transfer from core to
C	interference)		bypass stream
C_{D0}	profile (zero-lift) drag coefficient of the air-	η_o	overall efficiency of the engine
~	$\operatorname{craft} (C_{D0} = C_{D0,a} + C_{D0,e})$	η_p	propulsive efficiency
$C_{D0,i}$	profile (zero-lift) drag coefficient of the <i>i</i> th	η_t	isentropic efficiency of the turbine
	component of the airframe	η_T	thermal efficiency of the turbofan engine
C_f	skin friction coefficient	Θ	diameter
C_L	lift coefficient	Λ	wing sweep at leading edge
D	drag	ρ_a	density of air
$F_{\mathbf{N}}$	net thrust		
$\hat{F}_{ m N}$	specific net thrust		
$F_{ m N00}$	thrust at sea level static condition	Subscripts	
FF_i	interference form factor	Subscripes	•
g	acceleration due to gravity	2	at fan face
h'	gully height	2-class	2-class seating configuration
k	form factor	4	at entry to high pressure turbine
L	length	9	nozzle outlet
m	mass	abreast	abreast
\dot{m}	total mass flow rate of air through engine	bare	bare engine
\dot{m}_f	mass flow rate of fuel	BP	bypass cowl
\dot{M}	Mach number	cc	core cowl
MLW	maximum landing weight	cowl	cowl
N_c	Number of compressor stages	cr	cruise value
N_{en}	Number of engines	fan	engine fan
P^*	reference point from which interference form	fuse	fuselage
	factor is calculated	HT	horizontal tail
Pax	number of passengers	inc	incompressible
-	F 3.	-	r

installed bare engine combined with nacelle

max maximum nacelle nacelle op optimum pylon pylon

TAS true air speed VT vertical tail wing wing

Appendix 2

Calculation of maintenance cost

The AEA method²³ is followed for the determination of maintenance cost. The components of the maintenance costs depend on sea level static thrust (F_{N00} , tonnes), labour rate (R_L , \$/h), flight time (t_F , h), number of compressor stages (N_c), OPR and bypass ratio (B).

$$C_1 = 1.27 - (0.2B^{0.2}) (16)$$

$$C_2 = 0.4 \left(\frac{\text{OPR}}{20}\right)^{1.3} + 0.4 \tag{17}$$

$$C_3 = (0.032N_c) + 0.57 (18)$$

The labour cost for a single engine per hour of operation (LT) can be calculated from

$$LT = 0.21C_1C_3(1 + F_{N00})^{0.4}R_L (19)$$

The cost of material for a single engine per hour of operation is given by

$$MT = 2.56(1 + F_{N00})^{0.8}C_1(C_2 + C_3)$$
 (20)

Now, the maintenance cost of a single engine per flight can be calculated

$$EMC = (LT + MT)(t_F + 1.3)$$
 (21)

Appendix 3

Calculation of airframe profile drag coefficient

The equations used in this section are collated from Raymer, ²⁹ Kroo, ³⁰ Sommer and Short, ³¹ Avallone et al. ³² and Airbus UK. ³³ The airframe is divided into four main components: wing, fuselage, horizontal tail and vertical tail. The total airframe profile drag (zero-lift drag) is calculated by summing the profile drags of the individual components.

$$C_{D0,a} = \sum_{i=1}^{4} C_{D0,i} + C_{D0,misc}$$
 (22)

The first term in the RHS of equation (22) refers to the summation of the profile drag coefficients of the main components, and the second term $C_{D0,misc}$ consists of the summation of the profile drag coefficients of the belly fairing, flap tracks and other miscellaneous items. For each (*i*th) component, the profile drag $C_{D0,i}$ is calculated from the corresponding skin friction coefficient C_f from the relation

$$C_{D0,i} = kC_f \frac{S_{wet}}{S_{wing}} \tag{23}$$

where k is the form factor and S_{wet} the wetted area. How these are calculated for each of the four components have been indicated below.

For incompressible flow, the skin friction coefficient is given by Von Karman

$$C_{f,inc} = 0.455 \times [\log(Re)]^{-2.58}$$
 (24)

where the Reynolds number Re is calculated from

$$Re = \frac{\rho_a Vl}{\mu_a} \tag{25}$$

where l is a characteristic length. For the wing, $l = \text{MAC}_{wing}$; for the fuselage, $l = L_{fuse}$; for the horizontal tail, $l = \text{MAC}_{HT}$; for the vertical tail, $l = \text{MAC}_{VT}$. The viscosity of air μ_a is dependent on the prevailing temperature. The density ρ_a is to be determined at the appropriate altitude recognising air is compressible.

The incompressible skin friction coefficient has to be corrected for the compressibility effects. In fully turbulent flow, the wall temperature can be calculated from

$$\frac{T_w}{T_\infty} = 1 + 0.178 M_\infty^2 \tag{26}$$

The effective incompressible temperature and Reynolds Number are then defined by^{30,31}

$$\frac{T'}{T_{\infty}} = 1 + 0.035M_{\infty}^2 + 0.45\left(\frac{T_w}{T_{\infty}} - 1\right) \tag{27}$$

$$\frac{R'}{R_{\infty}} = \left(\frac{T_{\infty}}{T'}\right)^{2.5} \frac{T' + 216}{T_{\infty} + 216} \tag{28}$$

The compressibility corrected skin friction coefficient for each component is then calculated by

$$C_f = \left(\frac{T'}{T_{\infty}}\right)^{-1} \left(\frac{R'}{R_{\infty}}\right)^{-0.2} C_{f,inc} \tag{29}$$

k and S_{wet} for each of the four components are estimated as follows.

Wing. To attain a good estimation of the wing wetted area and the form factor, the thickness to chord ratio must be calculated

$$\left(\frac{t}{c}\right)_{70} = \left(0.90 - (M_{\infty} - 0.05)\cos\Lambda - \frac{1.23C_L}{10\cos^2\Lambda}\right)\cos\Lambda$$

$$k = 1 + \frac{2C(t/c)_{70}\cos^2\Lambda}{\sqrt{1 - M_{\infty}^2\cos^2\Lambda}} + \frac{C^2\cos^2\Lambda(t/c)_{70}^2(1 + 5\cos^2\Lambda)}{2(1 - M_{\infty}^2\cos^2\Lambda)}$$
(31)

where $Kroo^{30}$ recommends the value of the constant C = 1.1 for most realistic form factor calculation.

The wing wetted area is calculated with

$$S_{wet} = \left(1.977 + 0.52 \left(\frac{t}{c}\right)_{70}\right) \left(S_{wing} - c_r w_{fuse}\right)$$
 (32)

where SI units are used.

Fuselage. Kroo³⁰ outlines a method for calculating the fuselage form factor by calculating the maximum change in airspeed velocity over an ellipsoid. An arbitrary constant C = 2.3 gives a good match with experimental data³⁰

$$k = \left(1 + C\frac{\Delta U_{\text{max}}}{U_0}\right)^2 \tag{33}$$

$$\frac{\Delta U_{\text{max}}}{U_0} = \frac{\alpha}{(2 - \alpha) \times (1 - M^2)^{0.5}}$$
 (34)

$$\alpha = \frac{2 \times (1 - M^2) \times \delta^2}{\beta^3 (\tanh^{-1} \beta - \beta)}$$
 (35)

$$\delta = \frac{W_{fuse}}{L_{fuse}} \tag{36}$$

$$\beta = (1 - (1 - M^2)\delta^2)^{0.5} \tag{37}$$

The fuselage wetted area is assessed as being an open-faced cylinder

$$S_{wet} = \pi \cdot w_{fuse} \cdot L_{fuse} \tag{38}$$

Horizontal and vertical tails. The horizontal and vertical tail profile drags are calculated using a similar method to that of the wing, except the thickness to chord ratio is assumed to be 0.075 for form factor (k) calculations, and the wetted areas are calculated assuming the surfaces to be flat plates

$$S_{wet,HT} = 2(S_{HT} - \text{MAC}_{HT} \times w_{fuse})$$
(39)

$$S_{wet\ VT} = 2S_{VT} \tag{40}$$

Miscellaneous profile drag ($C_{D0,misc}$ in equation (22)). The profile drags of the belly fairing, flap tracks and other miscellaneous items are calculated by scaling the profile drags against those provided by Airbus for the A330-200.³³

Appendix 4

Calculation of profile drag coefficient of pylon and nacelle

The nacelle geometries for mixed flow and separate stream engines are estimated using methods outlined by Jenkinson et al.²⁶ These nacelle geometries are displayed in Figure 7.

The profile drag coefficient of the pylon and nacelle combination is calculated using equation (41)

$$C_{D0,e} = \frac{FF_i}{S_{wing}} \cdot \left(C_{f,cowl} \cdot S_{wet,cowl} + C_{f,pylon} \cdot S_{wet,pylon} \right)$$

$$\tag{41}$$

Interference form factor FF_i. The profile drag (zero-lift drag) of the nacelle and the pylon include the interference effect between them and the wing. In order to aid

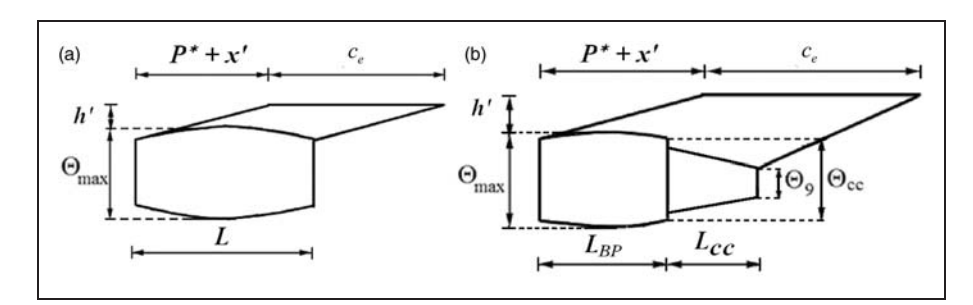


Figure 7. Nacelle and pylon geometry for (a) mixed stream engine (b) separate stream engine.

the process of calculating the interference form factor between the nacelle and the wing, Airbus³³ recommends the use of a defined location P^* (where P^* is a longitudinal distance from the leading face of the nacelle), the point from which the horizontal dimension x' is calculated, where x' represents the horizontal displacement between P^* and the leading edge of the wing.

For a mixed stream engine, P^* is at a point located two thirds along the length of the nacelle

$$P_{mixed}^* = \frac{2}{3}L\tag{42}$$

while for the separate stream engine, P^* is located at the trailing edge of the bypass cowl

$$P_{separate}^* = L_{BP} \tag{43}$$

For the FARE model, x' is calculated using equation (44)

$$x' = x_w - x_e - P^* + \left(y_e - \frac{1}{2}w_{fuse}\right)\tan\Lambda$$
 (44)

The gully height (h') between the underside of the wing and the top of the nacelle at the point of maximum diameter is also required in order to determine the magnitude of interference form factor. The gully height is equated to the vertical displacement by assuming that there is a low gradient at the trailing edge of the nacelle. This leads to a slight underestimation of the gully height, which in turn results in conservative values for the nacelle interference factor. The gully height is calculated by equation (45), where $z_{\rm max}$ is the maximum allowable displacement between the base of the nacelle and the underside of the wing (to maintain regulatory clearances, e.g. in the event of a nose gear collapse)

$$h' = z_{\text{max}} - \Theta_{\text{max}} \tag{45}$$

For the FARE model, once h' and x' are determined, the interference form factor (FF_i) can be calculated using data provided by Airbus, adapted in Figure 8. In the RARE model, on the other hand, h' and x' are chosen such that the interference form drag is minimised.

x' in the RARE model is chosen such that 20% of the local wing chord covers the nacelle and is given by equation (46)

$$x' = L - 0.2c_e - P^* (46)$$

Figure 8 is then used to determine the resulting gully height h' for the RARE model that minimises the interference form factor ($FF_i = 1$).

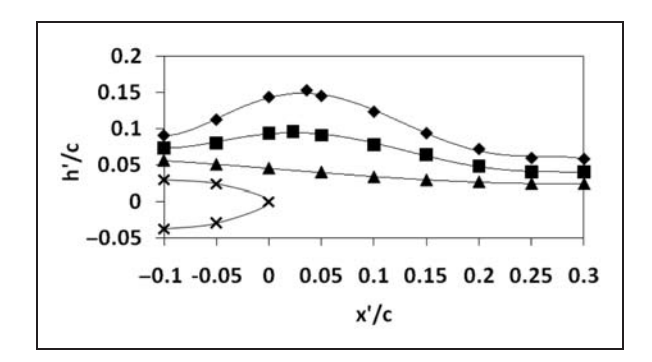


Figure 8. Determination of nacelle interference factor FF_i . Note: \times limit; \blacklozenge , \blacksquare and \triangle three different values of interference factor in order of increasing values starting from 1.0.

Calculation of C_f and S_{wet} in equation (41). Figure 7 displays the geometry of the nacelle and pylon structure, and shows the dimensions which are required for wetted area calculations in order to determine the nacelle and pylon profile drags. A complex (voluminous) set of equations given in Jenkinson et al.²⁶ has been adopted in this study to calculate all the dimensions shown in Figure 7, these equations are not reproduced here. The wetted areas are then calculated as follows

For mixed flow engines

$$S_{wet,cowl} = 0.9\pi\Theta_{\text{max}}L\tag{47}$$

$$S_{wet,nylon} = h'(c_e + L) \tag{48}$$

For separate stream engines

$$S_{wet,cowl} = 0.5\pi (\Theta_{\text{max}} + \Theta_{fan}) L_{BP} + 0.5\pi (\Theta_9 + \Theta_{cc}) L_{cc}$$
(49)

$$S_{wet,pylon} = (1.5c_e + 0.5(L_{BP} + L_{cc})) \times (h' - 0.5(\Theta_{max} - \Theta_{cc})) - 0.5L_{BP}(\Theta_{max} - \Theta_{cc})$$
(50)

The compressibility corrected values of $C_{f:cowl}$ and $C_{f:pylon}$ are calculated using equations analogous to equations (24) to (29) given in Appendix 3.

Appendix 5

Estimation of mass and dimensions of airframe and engine

In the development of a particular engine variant, scaling laws can be applied on the baseline engine to arrive at an initial design. For example, if the engine thrust scale, i.e. the ratio of required engine thrust and known engine thrust, is S_{thrust} , then the engine dimensions scale by the square root of the thrust scale ($S_{length} = \sqrt{S_{thrust}}$), engine mass and nacelle mass scale by thrust scale [$S_{mass} = S_{thrust}$]

i.e. the values of the ratios (engine thrust/engine mass) and (engine thrust/nacelle mass) remain constant], the fuel flow scales by thrust scale (i.e. sfc remains constant). These scaling laws are approximate but give a good indication of the mass and performance of a scaled engine at the preliminary design stage.

However, a rule of thumb is that thrust scaling should be limited to 20%. ²⁶ In the present context of developing a generic computer program covering all types of aircrafts and missions, however, mass and dimensions of engines have to be estimated over a large range of engine thrust and specific thrust. Hence, several empirical equations for functional relationships have been developed/used in this study.

Mass and dimensions of the engine and nacelle. The fan diameter (Θ_{fan}) of each modelled engine is calculated by the application of gas dynamics equations, considering the air mass flow rate required for the engines to operate at the cruise specific thrust of interest, the cruise atmospheric conditions and the fan entry Mach number. Once Θ_{fan} is known, functional relationships given in Jenkinson et al.²⁶ are used to determine all engine dimensions of the nacelle. Dimensions of the pylon and relations for positioning the engine are obtained from Airbus UK.³³ Please refer to Appendix 4.

A regression analysis has been performed on data covering 30 engines produced by Rolls Royce, General Electric, Pratt & Whitney and CFM International.⁵ Studies of these data show that the bare engine length can be predicted with good accuracy by scaling it from the fan diameter using

$$L_{bare} = 1.81\Theta_{fan} - 19.8 \tag{51}$$

where all values are in inches.

Further investigation suggests that the bare engine mass of each modelled engine can be found by applying factors to an effective volume term $L_{bare}\Theta_{fan}^2$

$$m_{bare} = 2.652 \left(L_{bare} \Theta_{fan}^2 \right)^{0.5833}$$
 (52)

Units: lbm and inches, where mass is in pounds and dimensions are in inches.

The nacelle mass is estimated using a method outlined by Raymer²⁹

$$m_{nacelle} = 0.6724 K_{ng} L_{nacelle}^{0.10} \ w_{nacelle}^{0.294} \ N_{z}^{0.119}$$

$$\times (2.331 m_{bare}^{0.901} K_{p} K_{tr})^{0.611} N_{en}^{0.984} S_{wet,nacelle}^{0.224}$$
(53)

where $K_{ng} = 1.017$, a factor to account for the fact that all nacelles of interest are pylon mounted, $N_z = 1.5 \times$ 'limit load factor' (where typical limit load factor = 3) = 4.5, $K_n = 1.0$, a factor showing that the

engines are turbofans, $K_{tr} = 1.18$ since the engines utilise reverse thrusters and $N_{en} =$ number of engines.

In equation (53), $m_{nacelle}$ is expressed in lbm, $L_{nacelle}$ and $w_{nacelle}$ in ft and $S_{wet,nacelle}$ in ft².

Having estimated the masses of the bare engine and the nacelle group, the installed engine mass can be calculated

$$m_{installed} = m_{bare} + m_{nacelle}$$
 (54)

Mass and dimensions of the RARE model airframe. The RARE model develops an airframe concurrently with the engine which is being optimised. All the airframe masses and dimensions are sized from relations derived from data describing aircraft which are currently produced by Airbus and Boeing.^{6,7} A regression analysis shows that the airframe mass can be estimated by equation (55), which relates the airframe mass to wing area, the design range and the number of passengers in a 2-class configuration

airframe mass (kg) =
$$207.8S_{\text{wing (m}^2)}$$

+ $6.5 \text{ range}_{\text{design (Nmi)}}$
+ $59.1pax_{2-\text{class}} - 17890$ (55)

The wingspan (b), root chord (c_r) , mean aerodynamic chord (MAC_{wing}) , spanwise engine location (y_e) , vertical tail area (S_{VT}) and horizontal tail area (S_{HT}) are sized from the wing area (S_{wing}) , while the fuselage length (L_{fuse}) and width (w_{fuse}) are scaled from the seating configuration and the number of passengers. These dimensions are used to calculate the airframe profile drag. Equations (56) to (63) show the relations derived from regression analysis

$$b = 3.77 \quad S_{wing}^{0.457} \tag{56}$$

$$c_r = 0.0169 \quad S_{wing} + 4.27 \tag{57}$$

$$MAC_{wing} = 0.0145 \quad S_{wing} + 2.13$$
 (58)

$$y_e = 0.150b + 0.775 (59)$$

$$S_{VT} = 0.136 \quad S_{wing} + 3.18 \tag{60}$$

$$S_{HT} = 0.25 \quad S_{wing} - 5.61$$
 (61)

$$w_{fuse} = 0.670 \quad Pax_{abreast} + 0.224$$
 (62)

$$L_{fuse} = 1.57 \left(\frac{Pax_{2-class}}{Pax_{abreast}} \right) + 0.924 \tag{63}$$

For landing gear mass, please refer to section 'Rubber aircraft mass' within the main text.